University of Thessaly

School of Engineering
Department of Mechanical Engineering

COUETTE FLOW OF MATERIALS WITH TEMPERATURE DEPENDENT VISCOSITY

by

Marina Konstantina Chaidi

Supervisor:

Dr. Athanasios Papathanasiou

Submitted in partial fulfillment of the requirements for the degree of Diploma in Mechanical Engineering at the University of Thessaly

Volos, 2023

University of Thessaly

School of Engineering
Department of Mechanical Engineering

COUETTE FLOW OF MATERIALS WITH TEMPERATURE DEPENDENT VISCOSITY

by

Marina Konstantina Chaidi

Supervisor:

Dr. Athanasios Papathanasiou

Submitted in partial fulfillment of the requirements for the degree of Diploma in Mechanical Engineering at the University of Thessaly

Volos, 2023

Approved by the Committee on Final Examination:

Advisor: Dr. Athanasios Papathanasiou
Professor, Department of Mechanical Engineering, University of Thessaly

Member: Dr. Georgios Charalampous
Assistant Professor, Department of Mechanical Engineering, University of Thessaly

Member: Dr. Andreas Tsiantis
Dr. Mechanical Engineering, Department of Mechanical Engineering, University of Thessaly

Date approved: [28/02/2023]

Acknowledgements

I would like to express my gratitude to my supervisor and professor Dr. Athanasios Papathanasiou, for his valuable assistance and guidance throughout the writing of this thesis. I am also very thankful to Mr. Andreas Tsiantis for his valuable support and advice during the implementation of this study on issues regarding to OpenFOAM software.

I would also like to thank Dr. Georgios Charalampous for being member of the examination committee and for reading my work.

Lastly, I am very grateful to my family and friends for being by my side and whose moral support played a significant role during the accomplishment of my studies.

COUETTE FLOW OF MATERIALS WITH TEMPERATURE DEPENDENT VISCOSITY

Marina Konstantina Chaidi

Department of Mechanical Engineering, University of Thessaly

Supervisor: Dr. Athanasios Papathanasiou

ABSTRACT

Couette flow can be found in many chemical, nuclear and mechanical engineering applications. Therefore, the correct computation of the flow is of great importance, especially when the fluid properties are functions of temperature. In this case, viscous forces are developed between the fluid elements leading to heat production. This phenomenon is known as viscous dissipation. In this thesis is investigated the circular Couette flow between two coaxial cylinders of materials with viscosity as polynomial function of temperature. Simulations of the flow are conducted using the CFD software OpenFOAM. Both geometrical parameters and material properties that affect the flow are examined. For this, were generated three different geometrical models based on the radius ratio of the cylinders. For each model are conducted simulations for a range of Br number values, obtaining the velocity and temperature profiles. The way that these parameters affect the flow is carefully analyzed. Lastly, the simulations results are compared in detail with series solutions up to second order in Br number for the velocity and third order for the temperature distribution.

Contents

List of Figures

1 INTRODUCTION

1.1 The Taylor-Couette Flow

The term Taylor-Couette describes the fluid flow between two concentric cylinders when the one, or both of them are rotating with a constant angular velocity. When the gap between the cylinders is small compared to the cylinder diameter, the term also refers to the flow between two parallel moving or stationary plates. The gap between the two surfaces is filled with an incompressible and usually highly viscous fluid. At low Reynolds numbers, therefore at low velocities, the flow is considered laminar and steady [1]. Regarding the viscosity and the thermal conductivity of the fluid, they can be functions of temperature or constants.

This flow was first investigated by Maurice Couette (1890) and it occurs in many chemical, nuclear and mechanical engineering applications. Couette flow is well known for its application in viscometry and rheological measurements. More particularly Couette flow can be found in many industrial applications as electric motors, rotating heat pipes, cooling of electrical systems, gas turbines as well as food and polymer processing industries. It is also applied in geothermal energy, cooling of nuclear reactors and gas drainage etc. In these cases both the viscosity and the thermal conductivity are functions of temperature [2].

Most of the devices that are employed in viscometry, lubrication and polymer industry, require that their design carefully considers the thermomechanical coupling between viscous heat generation and Couette flow. The development of viscous forces between the fluid elements leads to heat production, known as viscous-dissipation. When high viscosity fluids are subjected to shear, they can undergo a large increase in temperature due to viscous dissipation. This thermal development interacts with other destabilizing factors, including degradation or decomposition of the fluid, and reduces the functionality of the device. As a result, viscous heating is a common cause of error in viscometry, especially with rotational viscometers, where the entire sample is constantly sheared during the measurements. Therefore, a correct computation of the flow is crucial for the regular functioning of the device and especially the correct interpretation of its measurements [3].

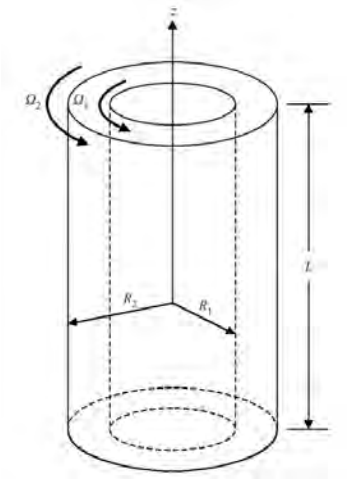

Figure 1.1: Schematic representation of Couette flow

1.2 History of Couette Flow Research

As R. Donelly said "Fluid caught between rotating cylinders has been intriguing physicists for over 300 years with its remarkably varied patterns and its chaotic and turbulent behaviour" [4]. Taylor-Couette flow refers mainly to the flow between two concentric cylinders when the one is rotating. This case, with the outer cylinder rotating, was first described by Maurice Couette in his thesis, which was presented at Paris in 1890 and it was mainly used as a viscometer. In 1923 G. I. Taylor studied the mathematical aspect of the case. For this, modern scientists named this type of flow Taylor-Couette flow [4].

Before Taylor, many approaches had been made to investigate the mathematical scope of the fluid motion between surfaces. Kelvin, Rayleigh [5] and many others have examined the flow between two infinite moving planar surfaces when the one moving relatively to other. Their objective was to specify the circumstances under which the flow is unstable. There appeared a divergence between the experimental results and theory as experiments with infinite surfaces was impractical. This problem led Taylor to examine the stability of a liquid between two cylinders. He concluded that below a critical value of the rotating velocity, the flow is laminar. Above this critical point the laminar flow is replaced by turbulence flow. The instability produces a continuous secondary motion in the form of vortices placed periodically along the cylinder's axis [6]. In 1928 J. Lewis's experiment validated Taylor's results [7].

The instability of Couette flow had been puzzling the scientific community in the following years. K. W. Schwartz et. al. [8] and D. Coles [9] considered the transition and the instabilities of the flow between two rotating cylinders in the presence of axisymmetric and non-axisymmetric disturbances, to determine the roots of the turbulence. They observed that the occurrence of Taylor vortices increases with the increase of the rotation velocity above the critical point, but eventually above a second critical point of speed the vortices acquire a 'wavy' form moving with a constant wave velocity.

In 1962 B. Gebhart [10] investigated the viscous dissipation effect in natural convection. He concluded that in the gravitational field of Earth, the dissipation is negligible for most typical engineering equipment. However, dissipation can be significant in circular systems. Furthermore, he observed that viscous dissipation cannot be ignored for rotating flows that can be described by high Prandtl numbers or flows in a high gravitational environment. Later, J. Nihoul [11] examined the flow of an incompressible fluid considering the viscosity and the thermal conductivity as functions of temperature. Nihoul proved that each Br number corresponded to a value of temperature and velocity, defining thus a unique profile of temperature, velocity as well as shear stress. In 1974 P. C. Sukanek et. al. [12] observed that above a critical value of Br number, there was a decrease of the shear stress when increasing the shear rate. Furthermore, T. D. Papathanasiou et. al. [13] investigated the thermomechanical coupling in circular Couette flow considering thermal conductivity and the viscosity as polynomial function of temperature. They compared the results of Numerical and Series solution for different values Br numbers and radius ratio of the cylinders.

1.3 State of the Art

Couette flow remains an interesting field of study due to the wide range of applications it encounters and the variety of the parameters by which it is affected. Particularly, the development of viscous dissipation and its effects are of great interest to the scientific community. G. C. Hazarika et. al. [14] and R. A. Kareem et. al. [15] investigated the flow of an incompressible fluid with variable viscosity and thermal conductivity, taking into consideration the impact of the magnetic field. They showed that an increase in viscosity caused an increase in the temperature and the wall shear stress profile but led to a decrease in the velocity profile. T. S. Yusuf et. al. [16] explored the entropy generation in a fluid flow between two infinite-length concentric cylinders in the presence of a radial magnetic field as well as viscous dissipation.

In the work of P. K. Mondal et. al. [17] regarding the influence of viscous heating

in flow through the annulus of two non-symmetrically heated concentric cylinders, the temperature profile was calculated for different values of Br number. Considering $Br = 0$ the temperature profile was linear as in the case of pure conduction, while for $Br > 0$ there was an increase in the fluid temperature. For $Br < 0$ the temperature decreased, as it concerned the cooling of the fluid. Similar results were obtained in the study of B. K. Jha et. al. [18] of the heat transfer in flow of a fluid with heat generating/absorbing properties, considering the effect of viscous dissipation.

S. Shabbir et. al. [19] conducted a thermal analysis of Couette flow within a small annulus. They proved that the velocity profile is linear for zero pressure gradient. Furthermore, they observed that the effect of viscous dissipation becomes more intense with the increase of Br number. Particularly, for $Br \approx 0$ the temperature profile is approximately linear, while as Br increases the profile becomes parabolic and the point of maximum temperature appears towards the centre of the distance between the cylinders. In the same year A. O. Ajibade et. al. [2] carried out a similar investigation, with additional consideration the boundary thickness, proving that it is another parameter that affects the flow and cannot be neglected.

1.4 Scope of this Study

As previously stated, Couette flow can be found in many chemical, nuclear and mechanical engineering applications. Of great interest is the heat generation due to viscous dissipation and the parameters that affect it.

The purpose of the present study is to examine the circular Couette flow of materials with temperature dependent viscosity. The flow is examined for different sizes of the gap between the two cylinders and different values of Br number. The main objective is the simulation of the flow, illustrating the viscous dissipation phenomenon, and the investigation of the parameters by which it is affected. The simulation's results for the velocity and temperature profiles, are compared with the series solutions proposed in the work of T. D. Papathanasiou et. al. [13].

The simulations of this work were carried out by using the Computational Fluid Dynamics (CFD) software OpenFOAM. The geometry and mesh structure were generated via the Gmsh software. For the validation of the solver that was used for the simulation, was considered the flow of material with constant viscosity. The simulations results were compared with the analytical solution. Since the range of solver's validity was determined, were carried out flow simulations of materials with temperature dependent viscosity, obtaining the velocity and temperature profile. The

proposed series solution were adapted in order to be compared to the simulations results. Finally, were examined the parameters that affect the flow and was conducted a comparison between the two solutions.

2 MATHEMATICAL FORMULATION OF COUETTE FLOW

As mentioned, Couette flow is the viscous fluid flow in the gap between two relatively moving boundaries. The flow is described by the Navier-Stokes equations, from which can be obtained the velocity and pressure profile. The temperature profile can be derived from the energy conservation equation. More precisely the governing equations of the flow are the following:

Conservation of Mass:

$$\frac{\partial \rho}{\partial t} + \nabla \cdot (\rho \mathbf{V}) = 0 \tag{2.1}$$

For incompressible fluid the density is constant and the equation is simplified:

$$\nabla \cdot \mathbf{V} = 0 \Rightarrow \frac{\partial u}{\partial x} + \frac{\partial v}{\partial y} + \frac{\partial w}{\partial z} = 0 \tag{2.2}$$

Conservation of Momentum:

$$\frac{\partial \rho \mathbf{V}}{\partial t} + \nabla \cdot (\rho \mathbf{V}\mathbf{V}) = -\nabla p + \nabla \cdot \tau + \mathbf{F} \tag{2.3}$$

Conservation of energy:

$$\frac{\partial}{\partial t}\left[\rho\left(e + \frac{1}{2}V^2\right)\right] + \nabla \cdot \left[\rho \mathbf{V}\left(e + \frac{1}{2}V^2\right)\right] = \nabla \cdot (k\nabla T) + \nabla \cdot (-p\mathbf{V} + \tau \mathbf{V}) + \mathbf{V} \cdot \mathbf{F} + Q \tag{2.4}$$

where $\mathbf{V}$ is the velocity field, $\mathbf{F}$ are the external forces that are applied to the fluid, Q is the amount of energy added to or removed from the system in the form of heat and τ is the stress tensor and for Newtonian fluids can be expressed as:

$$\tau = \mu\left(\nabla \mathbf{V} + \nabla \mathbf{V}^T\right) - \frac{2}{3}\mu \mathbf{I}\left(\nabla \cdot \mathbf{V}\right) \tag{2.5}$$

2.1 Plane Couette Flow

Considering the incompressible flow of a viscous fluid with constant density and thermal conductivity between two parallel plates, the one plate is moving with constant velocity while the other is stationary. Both plates maintain constant and uniform temperatures T_1 and T_2.

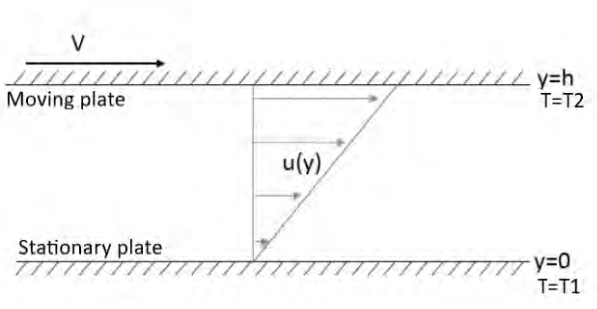

Figure 2.1: Plane Couette flow

Considering no slip boundary conditions:

$$u(x,0) = 0 \tag{2.6}$$

$$u(x,h) = V\,\frac{m}{s} \tag{2.7}$$

the equations (2.2) and (2.3) are simplified respectively to:

$$\frac{\partial v}{\partial x} = 0 \tag{2.8}$$

and

$$\mu\frac{\partial^2 u}{\partial y^2} = \frac{dp}{dx} \tag{2.9}$$

Therefore, the velocity profile is:

$$u(x,y) = \frac{1}{2\mu}\left(\frac{dp}{dx}\right)\left(y^2 - hy\right) + \frac{V}{h}y \tag{2.10}$$

The energy equation (2.4) for this flow can be expressed as:

$$\frac{\rho C_p dT}{dt} = k\nabla^2 T - T\left(\frac{\partial p}{\partial T}\right)\nabla\mathbf{V} + S \tag{2.11}$$

where S is the viscous heat generation term:

$$S = \mu\left(\frac{\partial u}{\partial y}\right)^2 \tag{2.12}$$

Applying the boundary conditions:

$$T(x,0) = T_1 \tag{2.13}$$

$$T(x,h) = T_2 \tag{2.14}$$

the temperature profile is:

$$\frac{T - T_1}{T_2 - T_1} = \frac{y}{h} + \frac{1}{2} Br \frac{y}{h} \left[1 - \frac{y}{h}\right] \tag{2.15}$$

where Br is the dimensionless Brinkman number, which is a measure of the heat conduction due to viscous dissipation:

$$Br = \frac{\mu u^2}{k(T_w - T_0)} \tag{2.16}$$

From the constitutive equation the shear stress can be expressed as:

$$\sigma = \mu \frac{du}{dy} = \mu \frac{V}{h} \tag{2.17}$$

2.2 Circular Couette Flow

Examining the flow of an incompressible viscous fluid between two coaxial cylinders. The inner cylinder of radius κR is stationary while the outer cylinder of radius R rotates with a constant angular velocity ω. Both cylinders maintain constant and uniform temperatures T_1 and T_2. The Reynolds number of the flow is defined as:

$$Re = \frac{\omega \kappa R(R - \kappa R)}{\nu} \tag{2.18}$$

where, $\nu = \frac{\mu}{\rho}$ the kinematic viscosity of the fluid. It is considered low Re number (approximately less than 2000), therefore steady-state laminar flow.

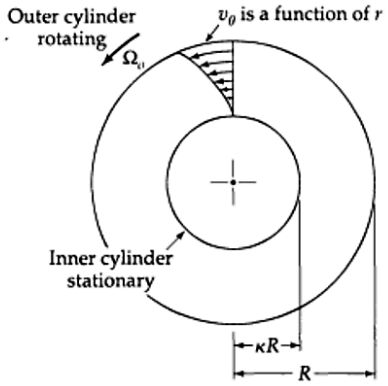

Figure 2.2: Circular Couette Flow

In the general case of variable viscosity and thermal conductivity, the momentum and energy equations that describe the flow can be formulated respectively as:

$$\frac{1}{x^2}\left[\frac{\partial}{\partial x}\left[\frac{\mu}{\mu_0}x^3\frac{\partial}{\partial x}\left(\frac{u}{x}\right)\right]\right]=0 \tag{2.19}$$

$$\frac{1}{x}\frac{\partial}{\partial x}\left[\frac{k}{k_0}x\frac{\partial\Theta}{\partial x}\right]+Br\frac{\mu}{\mu_0}\left[x\frac{\partial}{\partial x}\left(\frac{u}{x}\right)\right]^2=0 \tag{2.20}$$

where,

$$\Theta=\frac{T-T_0}{T_0},\ \ x=\frac{r}{R},\ \ u=\frac{u_\theta}{\omega R},\ \ Br=\frac{\mu_0(\omega R)^2}{k_0T_0} \tag{2.21}$$

In the equation (2.21), T_0 is a reference temperature, Br is the Brinkman number and μ_0, k_0 are known values for the viscosity and thermal conductivity, respectively. The equations (2.19), (2.20) can be further simplified in the case of constant viscosity or thermal conductivity.

From the equation (2.2), as shown in the following $u_r = 0$ at the boundaries, it appears that the only non-zero velocity is the u_θ:

$$\frac{\partial u_r}{\partial r}+\frac{u_r}{r}+\frac{1}{r}\frac{\partial u_\theta}{\partial\Theta}+\frac{\partial u_z}{\partial z}=0\Rightarrow\frac{1}{r}\frac{\partial}{\partial r}(ru_r)=0\Rightarrow u_r=0 \tag{2.22}$$

The velocity distribution can be calculated from the momentum conservation equation (2.3), considering constant properties and zero pressure gradient, as the flow arises from the rotation of the cylinders:

$$\frac{1}{r}\frac{\partial}{\partial r}\left(r\frac{u_\theta}{\partial r}\right)-\frac{u_\theta}{r^2}=0\Rightarrow u_\theta=c_1r+\frac{c_2}{r} \tag{2.23}$$

Applying the boundary conditions:

$$u_\theta(r=\kappa R)=0 \tag{2.24}$$

$$u_\theta(r=R)=\omega R \tag{2.25}$$

the final velocity profile of the flow is defined as follows:

$$u_\theta=\omega R\frac{\left(\frac{\kappa R}{r}-\frac{r}{\kappa R}\right)}{\left(\kappa-\frac{1}{\kappa}\right)} \tag{2.26}$$

Likewise, the temperature distribution as obtained from the energy equation, for the flow between two cylinders with constant uniform temperatures:

$$T(r)=\frac{T_1-T_2}{\ln\kappa}\ln\left(\frac{r}{R}\right)+T_2 \tag{2.27}$$

and the shear stress:

$$\tau_{r_\theta}=2\mu\omega R^2\left(\frac{1}{r^2}\right)\left(\frac{\kappa^2}{1-\kappa^2}\right) \tag{2.28}$$

2.3 An Approximate Series Solution For Circular Couette Flow

In this study is investigated the case of viscous dissipation, with the viscosity as a function of temperature and constant thermal conductivity. The analytical solution for this flow is obtained by the equations (2.19) and (2.20), where the equation (2.20) can be further simplified as follows:

$$\frac{1}{x}\frac{\partial}{\partial x}\left[x\frac{\partial \Theta}{\partial x}\right] + Br\frac{\mu}{\mu_0}\left[x\frac{\partial}{\partial x}\left(\frac{u}{x}\right)\right]^2 = 0 \tag{2.29}$$

The boundary conditions to be met in this case:

$$At\ \ x = \kappa:\ \ u = 0\ \ and\ \ \frac{\partial \Theta}{\partial x} = 0 \tag{2.30}$$

$$At\ \ x = 1:\ \ u = 1\ \ and\ \ \partial\Theta = 0 \tag{2.31}$$

The variation of viscosity with temperature can be expressed as:

$$\frac{\mu_0}{\mu} = 1 + \sum_{i=1}^{I} \beta_i \Theta^i \tag{2.32}$$

The solutions to the problem defined by the equations(2.19), (2.29) and the boundary conditions (2.30), (2.31) can be formulated as:

$$\frac{u(x)}{x} = u_0(x) + \sum_{n=1}^{N} u_n(x) Br^n \tag{2.33}$$

$$\Theta(x) = \Theta_0(x) + \sum_{n=1}^{N} \Theta_n(x) Br^n \tag{2.34}$$

In the work of T. D. Papathanasiou et. al. [13], [20], [21] and K. A. Caridis et. al. [22], are obtained solutions for the velocity and temperature profile, of second and third order in Br number.
More particular, the second-order solution for the velocity can be formulated as:

$$\frac{u(x)}{x} = u_0(x) + u_1(x)Br + u_2(x)Br^2 \tag{2.35}$$

where,

$$u_0(x) = \frac{\kappa^2 - x^2}{(-1+\kappa^2)x^2} \tag{2.36}$$

$$u_1(x) = \left[\frac{1}{x^2} - \frac{-1+\kappa^4-4\ln(x)-4\ln(x)\kappa^2}{\kappa^2(\kappa^2-1)}\right]\frac{\beta_1 C_0^3}{16x^2} + U_1 \tag{2.37}$$

with,

$$U_1 = \frac{\beta_1 C_0^3}{16}\left(\frac{\kappa^2-1-4\ln(\kappa)}{\kappa^2(-1+\kappa^2)}\right) \tag{2.38}$$

and

$$C_0 = \frac{2\kappa^2}{1-\kappa^2} \tag{2.39}$$

$$u_2(x) = u_{2\alpha}(x) + u_{2\beta}(x) + u_{2\gamma}(x) \tag{2.40}$$

where,

$$u_{2\alpha}(x) = \frac{C_0^5}{16}\left(\frac{-2\beta_2}{\kappa^4 x^2}\right)\ln(x)^2 \tag{2.41}$$

$$u_{2\beta}(x) = \left[\frac{\beta_2}{16}\left[\frac{2x^2\kappa^2-\kappa^2-2x^2}{x^4\kappa^4}\right] + u_{2\beta 1(x)}\beta_1^2\right]\ln(x)C_0^5 \tag{2.42}$$

with,

$$u_{2\beta 1} = -\frac{1}{32}\left[\frac{8x^2\ln(\kappa)+4x^2\ln(\kappa)\kappa^2-7x^2\kappa^2+6x^2+x^2\kappa^4-\kappa^2+\kappa^4}{\kappa^4x^4(-1+\kappa^2)}\right] \tag{2.43}$$

$$u_{2\gamma}(x) = -\frac{1}{384x^6}\left(u_{2\gamma 1}x^6 + u_{2\gamma 2}x^4 + u_{2\gamma 3}x^2 + u_{2\gamma 4}\right) \tag{2.44}$$

The $u_{2\gamma 1}$, $u_{2\gamma 2}$, $u_{2\gamma 3}$, $u_{2\gamma 4}$ coefficients are functions of the fluid properties and the radius ratio κ and can be found in the Appendix A.

The second-order solution for the temperature profile can be obtained as:

$$\Theta(x) = \Theta_0(x) + \Theta_1(x)Br + \Theta_2 Br^2 \tag{2.45}$$

For an isothermal system, the viscosity is constant and the $Br = 0$, therefore in the equation (2.45) the term $\Theta_0(x) = 0$. The terms $\Theta_1(x)$ and $\Theta_2(x)$ can be expressed as:

$$\Theta_1(x) = \left[-\frac{2\ln(x)-\kappa^2}{4\kappa^2} - \frac{1}{4x^2}\right]C_0^2 \tag{2.46}$$

and

$$\Theta_2(x) = F_1\ln(x) + F_2 \tag{2.47}$$

where,

$$F_1(x) = \frac{C_0^4}{16}\left[\frac{[(4\ln(\kappa) + 4\ln(\kappa)\kappa^2 - 3\kappa^2 + 3)\beta_1]\, x^2 + 2\kappa^2(\kappa^2 - 1)\beta_1}{\kappa^4 x^2(-1 + \kappa^2)}\right] \tag{2.48}$$

and

$$F_2(x) = C_0^4\left(\frac{x^2 - 1}{\kappa^2 - 1}\right)\left[\frac{(4x^2 - 5x^2\kappa^2 + x^2\kappa^4 + 16x^2\ln(\kappa) - \kappa^2 + \kappa^4)\beta_1}{-64\kappa^2 x^4}\right] \tag{2.49}$$

For a more accurate temperature profile can be obtained a third-order solution as:

$$\Theta(x) = \Theta_1(x)Br + \Theta_2(x)Br^2 + \Theta_3(x)Br^3 \tag{2.50}$$

The form of $\Theta_3(x)$ is considerably more complex and can be found in the study of T.D. Papathanasiou [13].

3 FLOW SIMULATIONS USING OpenFOAM

In the present work the simulations of the flow were performed by using the software OpenFOAM, an open source tool for Computational Fluid Dynamics (CFD). The advantage of this software is the free access and the variety of features used to simulate demanding fluid flows including heat transfer, turbulence and even chemical reactions. The file structure of OpenFOAM simulations consist of three main directories: the system, the constant and the time directories, as presented in the figure 3.1.

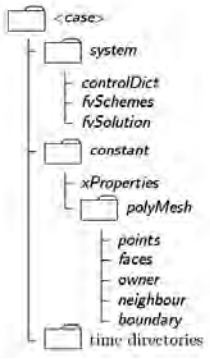

Figure 3.1: File structure of OpenFOAM simulations

The system directory consists of three main files, which should be included in any OpenFOAM case; the *controlDict*, *fvSchemes* and *fvSolution* files. The simulation's general operation is managed by the *controlDict* file. In the *fvSchemes* file are specified the numerical schemes used for the terms in the problem's governing differential equations. Each governing equation is solved by a numerical solver as defined in the *fvSolution* file. In the *constant* directory are contained two main files defining the thermophysical properties of the fluid and the turbulence properties of the flow. More particular, in the *thermophysicalProperties* file can be specified the thermophysical modelling of the simulation, through the *thermoType* dictionary item. In the *constant* directory is also contained the *polyMesh* folder in which can be found the files that describe the geometry and the mesh structure. In the *0* time directory are defined the boundary conditions and the initial values for each variable of the case.

For the purpose of this study where used two different solvers, the simpleFoam and rhoSimpleFoam solver.

3.1 SimpleFoam

SimpleFoam is a solver for steady-state, incompressible and turbulent flow. The algorithm that is used is the SIMPLE (Semi-Implicit Method for Pressure Linked Equations) or the SIMPLEC (Semi-Implicit Method for Pressure Linked Equations Consistent) algorithm. The following strategy is used for the solution: The equations describing the flow are solved sequentially and the each solution is applied to the following equation.
More particular, at first is solved the momentum equation:

$$\frac{\partial u_{rj} u_i}{\partial x} + \epsilon_{ijk}\omega_i u_j = -\frac{1}{\rho}\frac{\partial p}{\partial x_i} + \frac{1}{\rho}\frac{\partial}{\partial x_j}(\tau_{ij} + \tau_{tij}) \tag{3.1}$$

where, u is the absolute velocity, u_r is the relative velocity, ω is the angular velocity and τ_{ij}, τ_{tij} represent the viscosity and turbulence stress, respectively. From this solution is derived a velocity field which is a function of pressure and satisfies the momentum equation but not the continuity equation. This field is inserted in the continuity equation and is obtained a pressure profile, which is added in the momentum equation. The above procedure is continued until convergence. Eventually, arises a velocity profile satisfying both equations.[23]

In this study simpleFoam was used for the simulation of a steady-state laminar Couette flow between two cylinders, with constant fluid properties. The velocity profile obtained and the solution was compared with the analytical solution.

3.2 rhoSimpleFoam

RhoSimpleFoam is a solver for steady-state, compressible and turbulent flow. As in simpleFoam, the algorithm that is used is SIMPLE or SIMPLEC algorithm. The solution strategy is similar with simpleFoam strategy. The difference arises from the fact that in compressible flow density varies with the temperature and it leads to the addition of the energy equation.
More precisely, the momentum equation is expressed for a moving reference frame as:

$$\nabla \cdot (\rho \mathbf{u_r} \times \mathbf{u_I}) + \rho\boldsymbol{\omega} \times \mathbf{u_I} = \nabla p + \nabla \cdot (\mathbf{R_{vis}} + \mathbf{R_{tur}}) \tag{3.2}$$

where, $\mathbf{u_R}$ is the relative velocity, $\mathbf{u_I}$ is the velocity in the inertial frame, $\boldsymbol{\omega}$ is the angular velocity of the rotational frame and $\mathbf{R_{vis}}$, $\mathbf{R_{tur}}$ are the stress tensors due to viscosity and turbulence, respectively. The energy equation to be solved is:

$$\frac{\partial}{\partial t}(\rho e_t) + \nabla \cdot (\rho e_t \mathbf{u} + \mathbf{u}p + \mathbf{q_{vis}} + \mathbf{q_{tur}} - \mathbf{R_t} \cdot \mathbf{u} - \mathbf{R_{vis}} \cdot \ddot{\mathbf{u}} - 0.5\rho\ddot{\mathbf{u}}(\ddot{\mathbf{u}} \cdot \ddot{\mathbf{u}})) = 0 \tag{3.3}$$

where e_t is the total energy, defined as:

$$e_t = e + 0.5\mathbf{u} \cdot \mathbf{u} + k \tag{3.4}$$

the term k represents the turbulent kinetic energy.
As mentioned rhoSimpleFoam is a solver for steady-state flows, therefore in the equation (3.3) the time derivative is equal to zero. In addition, considering laminar flow, the turbulent kinetic energy and the last terms of the equation (3.3) can be neglected and the energy equation is simplified:

$$\nabla \cdot ((\rho(e + 0.5\mathbf{u} \cdot \mathbf{u})\mathbf{u} + \mathbf{u}p + \mathbf{q_t}) = 0 \tag{3.5}$$

where $\mathbf{q_t}$ is the total heat flux defined as the sum of heat flux due to viscosity and turbulence, as follows:

$$\mathbf{q_t} = \mathbf{q_{vis}} + \mathbf{q_{tur}} \tag{3.6}$$

and it is calculated as:

$$\mathbf{q_t} = -\frac{\mu}{Pr}\frac{c_p}{c_v}\nabla e \tag{3.7}$$

By inserting the enthalpy definition:

$$h = e + \frac{p}{\rho} \tag{3.8}$$

the equation (3.5) is formulated as:

$$\nabla \cdot ((\rho(h + 0.5\mathbf{u} \cdot \mathbf{u})\mathbf{u} + \mathbf{q_t}) = 0 \tag{3.9}$$

In the case that is chosen the sensible enthalpy the total heat flux can be calculated as:

$$\mathbf{q_t} = -\frac{\mu}{Pr}\nabla h \tag{3.10}$$

Where Pr is the dimensionless Prandtl number, defined as the ratio of momentum diffusivity (kinematic viscosity) to thermal diffusivity and can be expressed as:

$$Pr = \frac{v}{\alpha} = \frac{c_p \mu}{k} \tag{3.11}$$

In this study rhoSimpleFoam was used for a steady-state, laminar circular Couette flow simulation of an incompressible fluid, with temperature dependent viscosity and constant thermal conductivity. The solution is compared with the analytical solution as obtained in the work of T.D. Papathanasiou et. al. [13]. For this aim it was required defining the viscosity as a polynomial function of temperature in the *thermophysicalProperties* directory. The thermophysical modelling package that was used for the simulation is described in the figure 3.2.

```
thermoType
{
    type            heRhoThermo;
    mixture         pureMixture;
    transport       polynomial;
    thermo          hPolynomial;
    equationOfState icoPolynomial;
    specie          specie;
    energy          sensibleInternalEnergy;
}
```

Figure 3.2: thermoType package

More particular, the *polynomial transport* requires the viscosity to be expressed as a polynomial function of temperature of any order:

$$\mu = \sum_{i=0}^{N-1} a_i T^i \tag{3.12}$$

The coefficients a_i are also specified in the *thermophysicalProperties* directory.

As previously stated, by using rhoSimpleFoam are solved the energy equation along with the momentum equation. In the case of variable viscosity the term of heat generation due to viscous dissipation must be considered in the energy equation. This additional source term is specified in the *fvOptions* file which is contained in the *system* directory, as described in the figure 3.3.

```
viscousD1
        {
            type            viscousDissipation;
            enabled         true;

            viscousDissipationCoeffs
            {
                fields      (T);
                rho         rho;
            }
        }
```

Figure 3.3: Adding the viscous dissipation term

3.3 Adaptation of the Series Solution for OpenFOAM simulations

In this study is performed a comparison between the simulation results with the series solution described in section 2.3. For this, is required a modification of the equation (2.32) so it is comparable to the equation (3.12). The original model for viscosity (2.32) can be expressed as:

$$\frac{\mu}{\mu_0} = \frac{1}{1 + \beta_1\Theta + \beta_2\Theta^2 + \beta_3\Theta^3} \tag{3.13}$$

To specify the problem, is considered: $\beta_1 = 1$, $\beta_2 = 0.5$ and $\beta_3 = 0.25$.
The equation (3.13) can be approximated, with high accuracy, by the following polynomial function:

$$\frac{\mu}{\mu_0} = 1 + \sum_{i=0}^{7} c_i\Theta^i \tag{3.14}$$

where, $c = (0 \quad -1 \quad 0.5 \quad -0.25 \quad 0.25 \quad -0.25 \quad 0.188 \quad -0.125)$. The c_i coefficients are calculated in the Appendix B.
In figure 3.4 is presented the comparison between the original model for viscosity and the polynomial approximation. The x-axis refers to the non-dimensional temperature Θ and the y-axis to the ratio $\frac{\mu}{\mu_0}$. The dotted line indicates the original model, described by the equation (3.13) and the red line to the model described by the polynomial function (3.14).

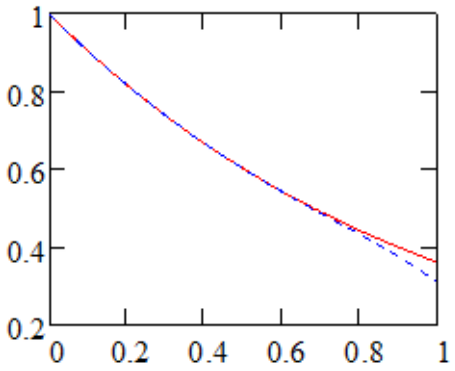

Figure 3.4: Viscosity model comparison

The non-dimensional temperature can be expressed as:

$$\Theta = \frac{T - T_0}{T_0} \Rightarrow T = T_0(\Theta + 1) \tag{3.15}$$

By adding the equation (3.15) in the equation (3.14) is obtained the viscosity as a function of the dimensional temperature:

$$\frac{\mu}{\mu_0} = \sum_{i=0}^{7} d_i T^i \tag{3.16}$$

The equation (3.16) can be approximated with high accuracy by a third-order solution:

$$\frac{\mu}{\mu_0} = \sum_{i=0}^{3} d_i T^i \tag{3.17}$$

where, $d = (2.75 \quad 0.0080882353 \quad 0.0000108131 \quad 0.000000006361)$
By multiplying the coefficients d_i by the reference viscosity μ_0 can be obtained the coefficients a_i of the equation (3.12).
The viscosity model described by the equation (3.16) is presented in the figure 3.5.

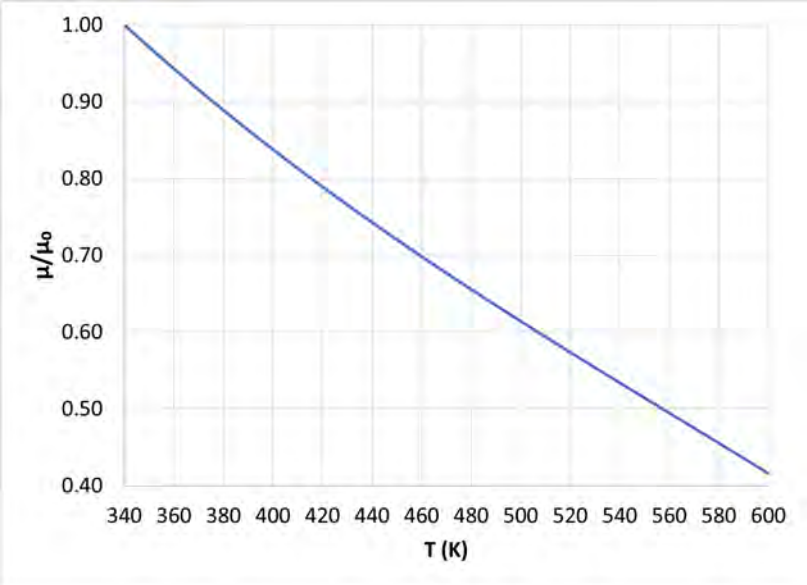

Figure 3.5: Viscosity model as function of temperature

4 GEOMETRY AND MESH STRUCTURE

The geometry and the mesh used for the simulations where generated via the Gmsh software. Gmsh is an open source software for 3D finite element mesh generation that includes a CAD engine. It consist of four modules: geometry designing, mesh structure, solver and post-processing. The advantage of this tool is the fast meshing, its user friendly environment and the capability of parametric inputs [24].

As already described, in this study is examined the circular Couette flow for three different values of the cylinders radius ratio κ. Therefore there was generated different meshes for each value of the radius ratio. For this aim, the coordinates for the geometry design and the mesh structure were defined as variables, which values are determined by the user as shown in the figure 4.1.

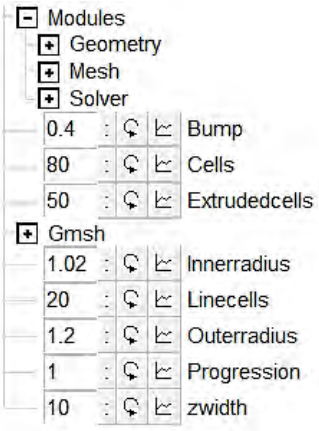

Figure 4.1: Setting variables in Gmsh (indicative values)

In the table 1 are presented the radius values of the outer and inner cylinders for the three different values of κ. The length of the cylinders is considered 1m.

κ	0.5	0.75	0.85
inner radius (cm)	6	9	10.2
outer radius (cm)	12	12	12

Table 1: Cylinders radius for different κ values

Both 2D and 3D meshes were created. Firstly, the 3D mesh was used for the flow simulation of a fluid with constant properties. The flow that is examined is laminar,

thus it can be considered as two-dimensional. Therefore, in the interest of time saving, it was created a 2D mesh, used for the flow simulation of a fluid with temperature dependent viscosity. In all cases the mesh was structured (*transfinite* command) and was thicker near the boundaries (*bump* command) in order to ensure higher accuracy, faster generation and uniform distribution of the cells.

In the case of 3D the mesh was consisted of 300200 cells (hexahedra). In the figures 4.2, 4.3 and 4.4 is presented the mesh for the different values of κ.

(a) (b)

(c)

Figure 4.2: 3D mesh for $\kappa = 0.85$

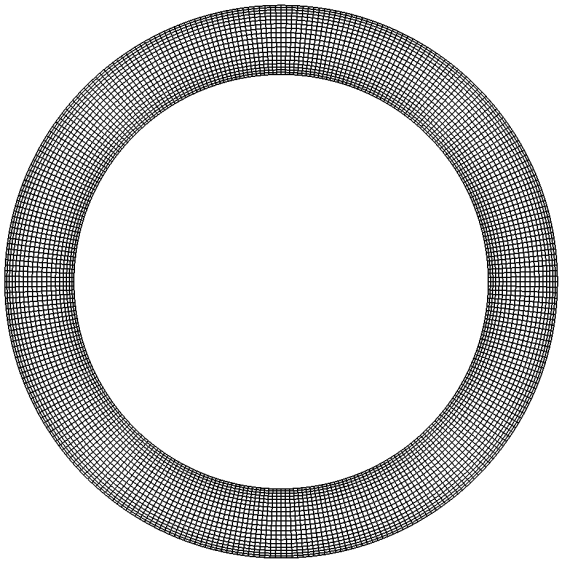

(a)

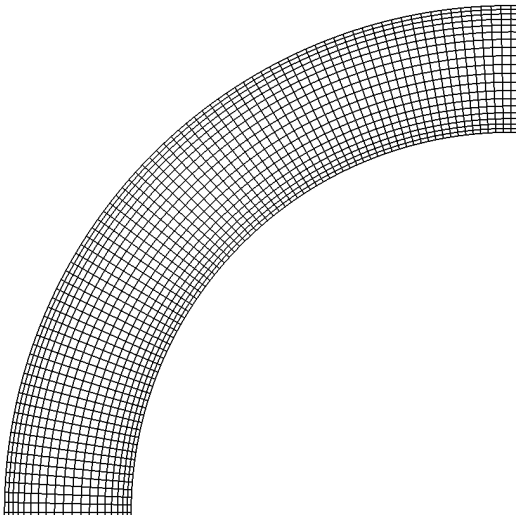

(b)

(c)

Figure 4.3: 3D mesh for $\kappa = 0.75$

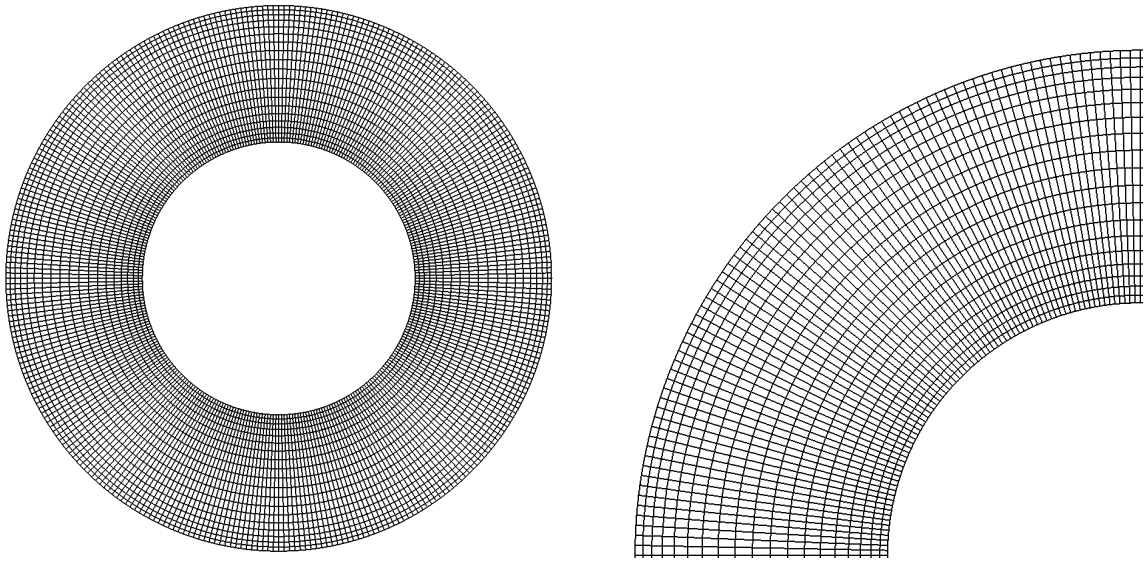

(a) (b)

(c)

Figure 4.4: 3D mesh for $\kappa = 0.5$

In the case of 2D the mesh thickness along the z-direction consisted of one cell. In the table 2 is presented the number of the mesh cells (hexahedra) for each value of radius ratio κ.

κ	0.5	0.75	0.85
number of cells	18564	18564	9044

Table 2: Number of cells for each value of κ

In the figures 4.5, 4.6 and 4.7 is presented the mesh structure for each case of κ value.

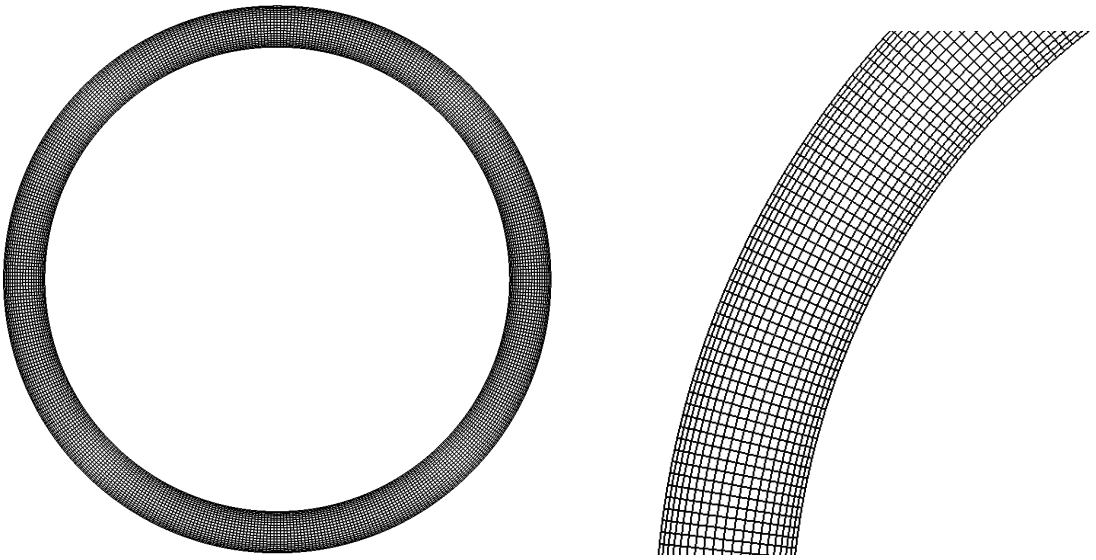

(a) (b)

Figure 4.5: 2D mesh for $\kappa = 0.85$

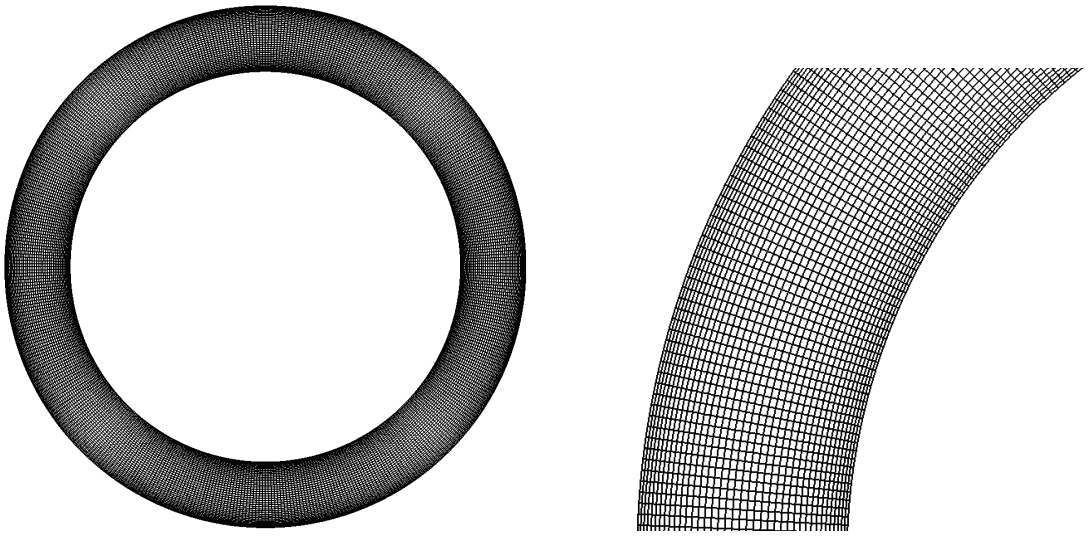

(a) (b)

Figure 4.6: 2D mesh for $\kappa = 0.75$

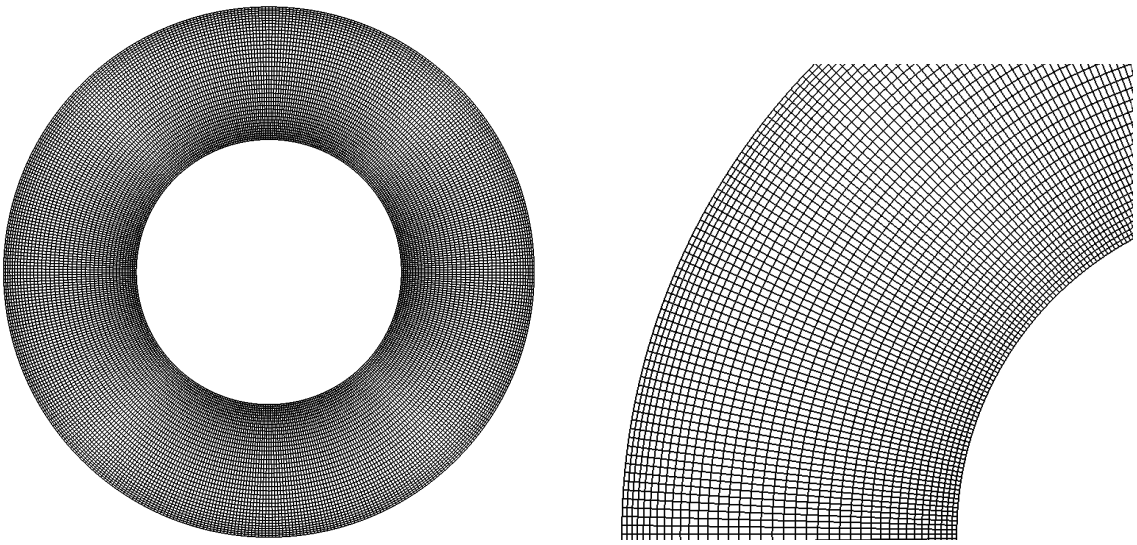

(a) (b)

Figure 4.7: 2D mesh for $\kappa = 0.5$

5 RESULTS

In this study is examined the circular Couette flow for three different values of the cylinders radius ratio κ. Firstly, is obtained the velocity profile, for the simple case of constant viscosity and thermal conductivity, without the effect of temperature variation. Then is investigated the case of viscous dissipation, with the viscosity as a function of temperature and constant thermal conductivity. In this section are presented the results of the simulations for the velocity and temperature profile and their comparison with the analytical solution as described in the section 2.

5.1 Couette Flow Simulation of Materials with Constant Viscosity

As previously stated, in the present work is firstly examined the flow of a material with constant properties. This simulation carried out using simpleFoam solver. In this case are considered two coaxial cylinders where the outer one is rotating with constant velocity $4\,rad/s$. In order to ensure low Re number, therefore laminar flow, the viscosity is determined equal to $\mu_0 = 0.1\,Pa \cdot s$. There are used 3D mesh structures, as described in section 4. The obtained velocity profile is compared to the profile given by the equation (2.26). Furthermore, is investigated the profile's divergence from the linear profile. In the figure 5.1 is presented the velocity profile for each value of the radius ratio κ, as obtained from the OpenFOAM simulations.

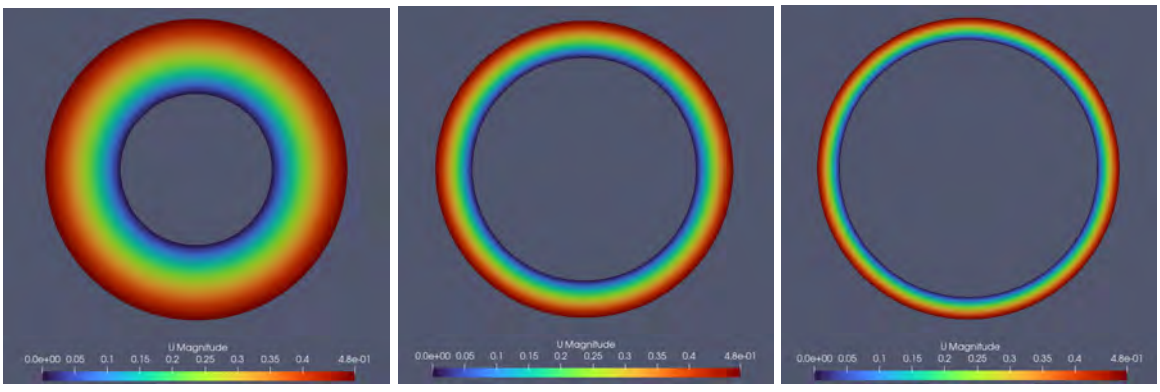

(a) $\kappa = 0.5$ (b) $\kappa = 0.75$ (c) $\kappa = 0.85$

Figure 5.1: Velocity profile for each value of κ. In the legend the minimum velocity is $0m/s$, the maximum is $0.48m/s$ and the scaling is $0.05m/s$.

In the figures 5.2, 5.3 and 5.4 is presented the comparison of the velocity profiles for the different values of the radius ratio κ. Where, the y-axis refers to the velocity $u_\theta(m/s)$ and the x-axis to the distance between the two cylinders. The blue line indicates the velocity profile as obtained from the OpenFOAM simulations and the black dotted line the profile as obtained from the analytical solution (2.26). The dotted grey line represents the linear profile.

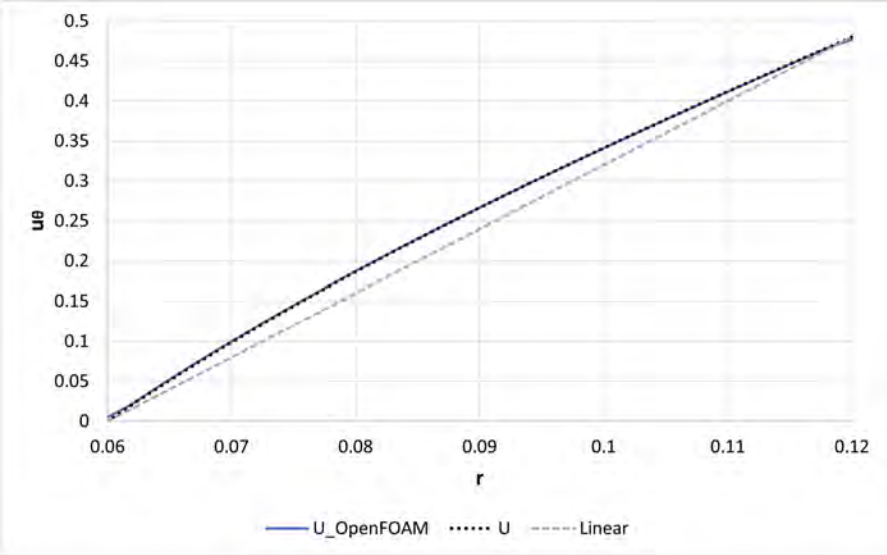

Figure 5.2: Velocity profile comparison for $\mu_0 = 0.1Pa \cdot s$ and $\kappa = 0.5$

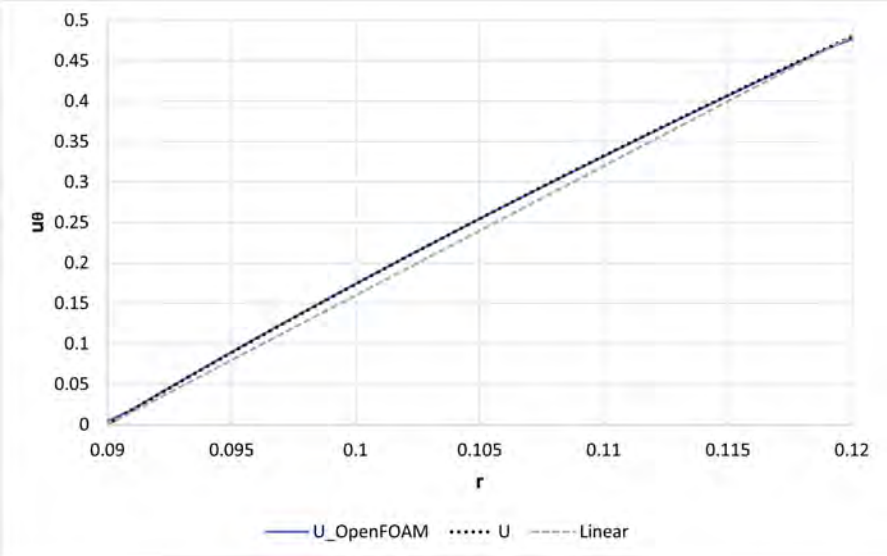

Figure 5.3: Velocity profile comparison for $\mu_0 = 0.1Pa \cdot s$ and $\kappa = 0.75$

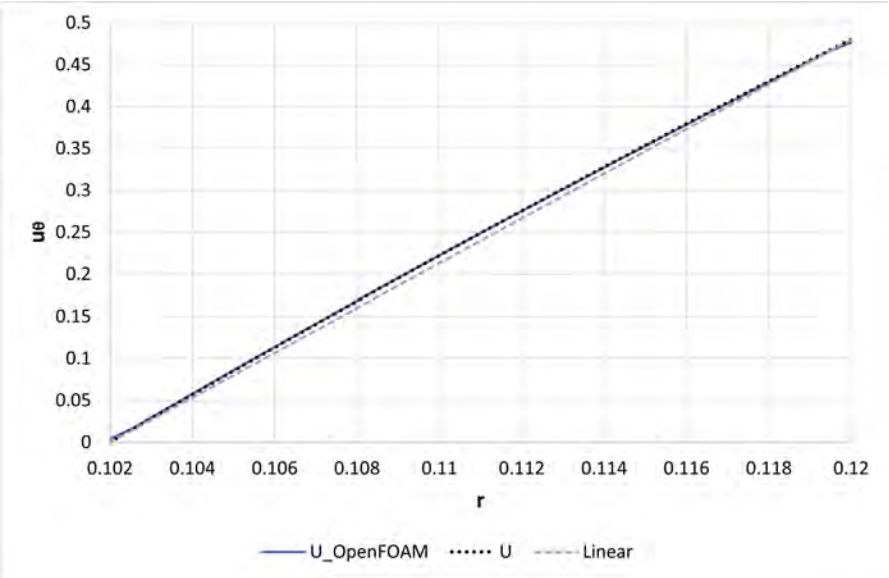

Figure 5.4: Velocity profile comparison for $\mu_0 = 0.1 Pa \cdot s$ and $\kappa = 0.85$

From the above comparison, it can be observed that the profiles derived from the simulation and the analytical solution are fully identical. Thus, is ensured the validity of the simulation's results. Most importantly it can be shown that when the gap between the cylinders is small compared to the cylinder diameter, the velocity profile is sufficiently approximating the linear profile. As the gap increases the velocity profile becomes parabolic.

5.2 Validation of rhoSimpleFoam solver

As stated in section 3, the flow simulations of materials with temperature dependent viscosity carried out using rhoSimpleFoam solver. Therefore, was required the validation of the solver. For this aim, is performed a comparison between the simulation's results and the analytical solution given by the equations (2.26) and (2.27). In this case is considered that both inner and outer cylinder maintain constant temperature $340K$ and $341K$, respectively. As in the simpleFoam case, in order to ensure laminar flow, the outer cylinder is rotating with constant velocity $4\, rad/s$ and the material's viscosity is constant $\mu_0 = 0.1\ Pa \cdot s$, therefore $Br = 0$. Furthermore, 2D meshes are used for the simulation, as stated in section 4.

In the figures 5.5, 5.6 and 5.7 is presented the comparison of the velocity profiles, as

obtained from the simulations and the analytical solution (2.26), for each value of the radius radio κ. Where, the y-axis refers to the velocity $u_\theta(m/s)$ and the x-axis to the distance $r(m)$ between the two cylinders. The blue line indicates the velocity profile as obtained from the OpenFOAM simulations and the black dotted line the profile as obtained from the analytical solution (2.26). The dotted grey line represents the linear profile.

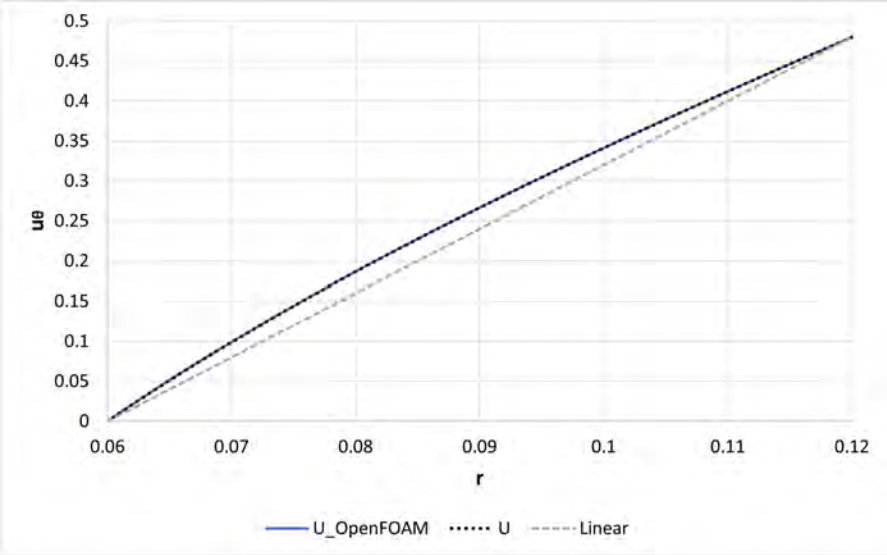

Figure 5.5: Velocity profile comparison for $\kappa = 0.5$

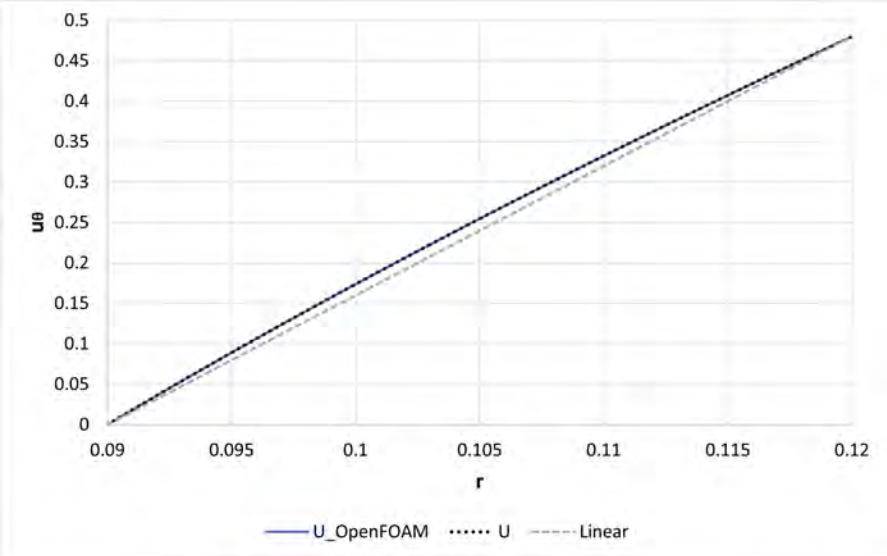

Figure 5.6: Velocity profile comparison for $\kappa = 0.75$

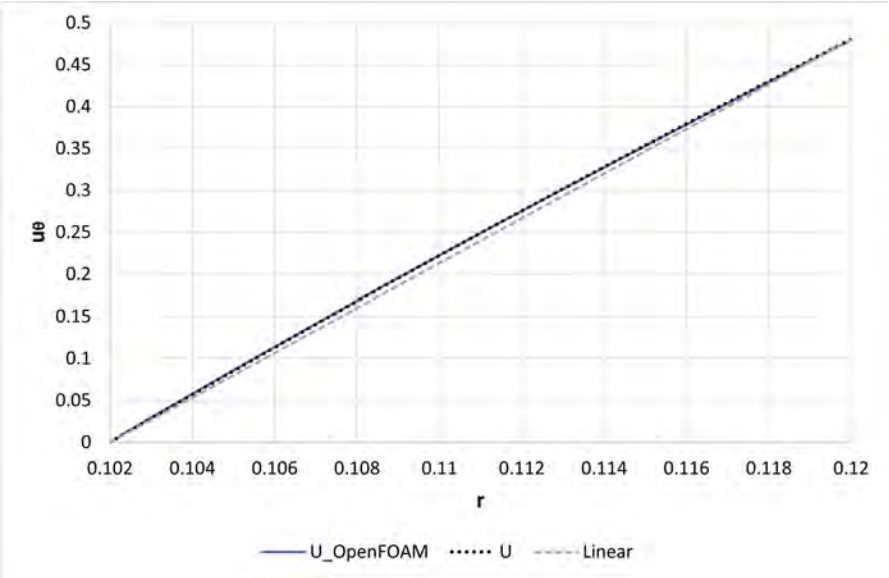

Figure 5.7: Velocity profile comparison for $\kappa = 0.85$

In the figures 5.8, 5.9 and 5.10 is presented the comparison of the temperature profiles, as obtained from the simulations and the analytical solution (2.27), for each value of κ. Where, the y-axis refers to the temperature $T(K)$ and the x-axis to the distance $r(m)$ between the two cylinders. The blue line indicates the velocity profile as obtained from the OpenFOAM simulations and the black dotted line the profile as obtained from the analytical solution (2.27).

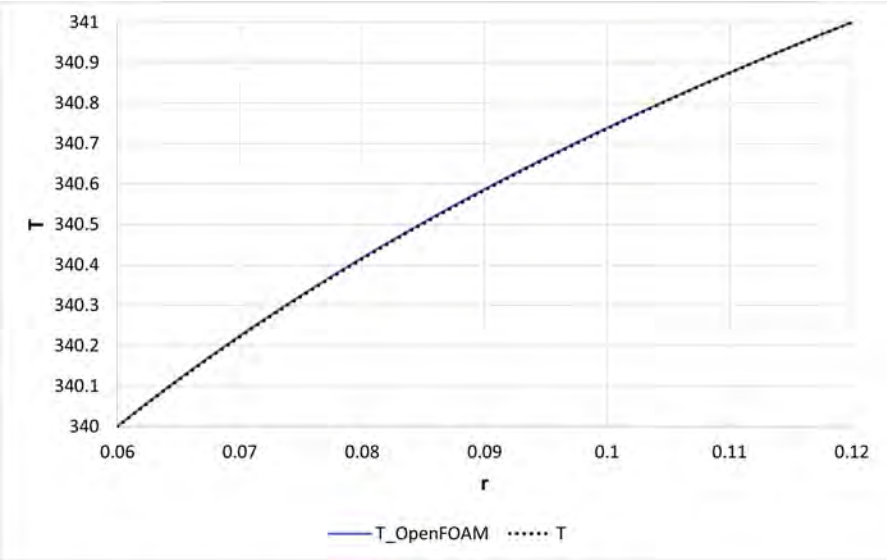

Figure 5.8: Temperature profile comparison for $\kappa = 0.5$

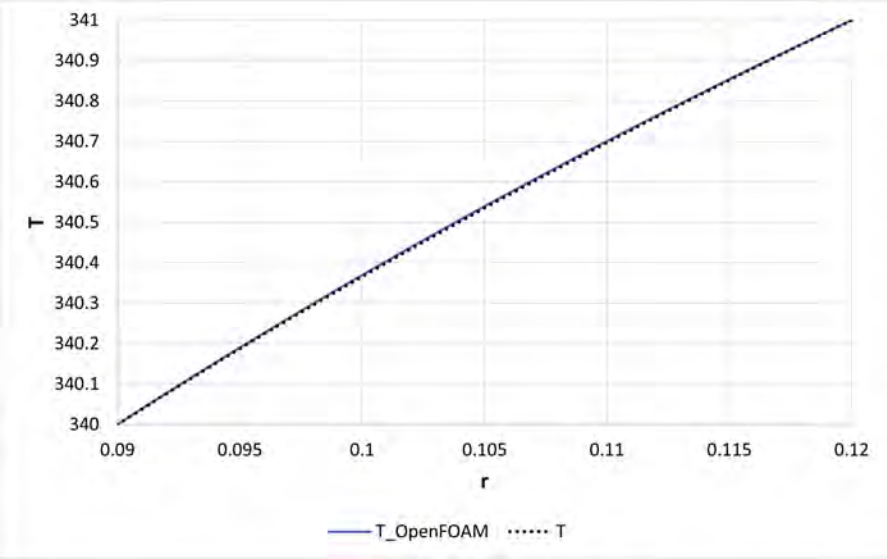

Figure 5.9: Temperature profile comparison for $\kappa = 0.75$

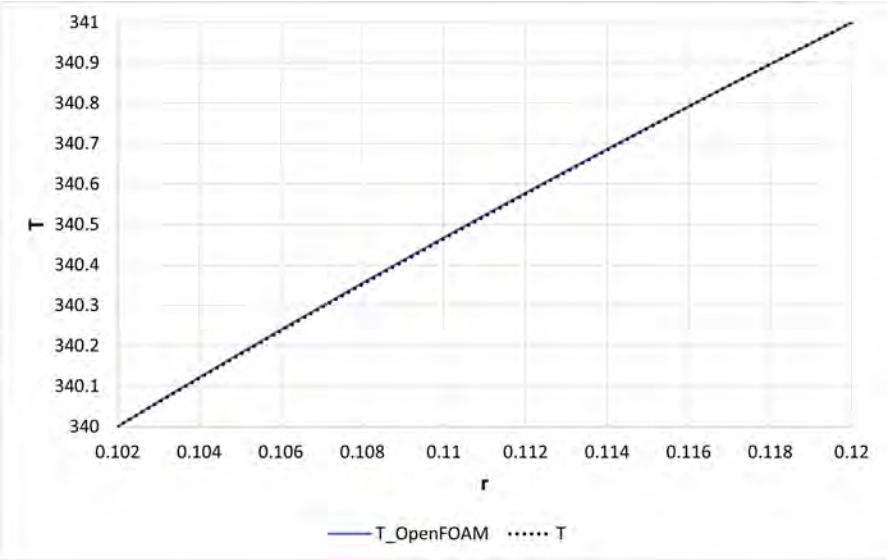

Figure 5.10: Temperature profile comparison for $\kappa = 0.85$

From the above comparison, it can be shown that the velocity and temperature profiles obtained from the simulation are completely similar to the profiles derived from the analytical solution. The conclusion to be drawn is that rhoSimpleFoam is suitable for the simulations of this study, as highly accurate results can be obtained. Since the validity of rhoSimpleFoam is determined it can also be used for the Couette flow simulations of materials with temperature dependent viscosity.

5.3 Viscosity as Function of Temperature

In this case is considered the circular Couette flow of materials with viscosity as a function of temperature described by the equation (3.17). The outer cylinder is rotating with constant velocity $4rad/s$ and maintains constant temperature $340K$, while the inner is stationary. Regarding to the temperature, at the inner cylinder is applied zero Gradient boundary condition, simulating the case of a thermally insulated inner cylinder. The mathematical model of the examined case is described in detail in section 2.3.

As shown, the velocity and temperature distribution are depending from both geometrical parameters and material properties. Therefore, were carried out flow simulations for different values of the radius ratio κ and the Br number.
In the figures 5.11, 5.12 and 5.13 is presented the temperature profile for radius ratios $\kappa = 0.5$, $\kappa = 0.75$ and $\kappa = 0.85$ and Br number values ranging from 0.5 to 2, as obtained from the OpenFOAM simulations.

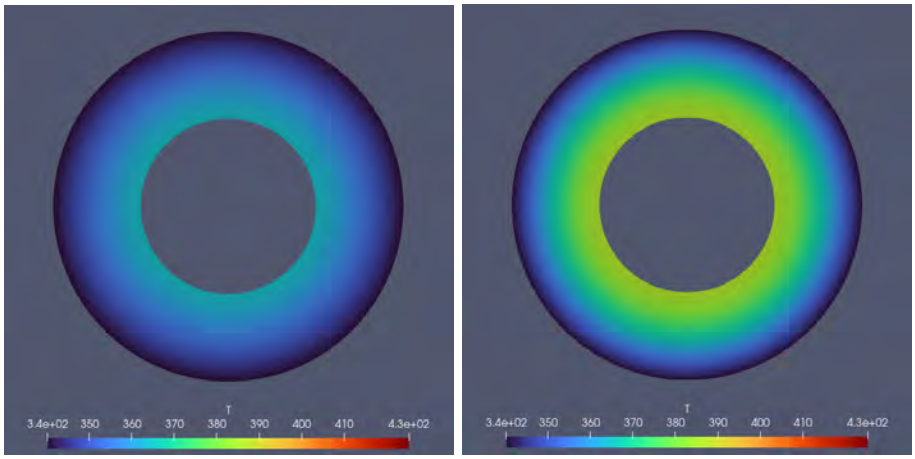

(a) $Br = 0.5$ (b) $Br = 1$

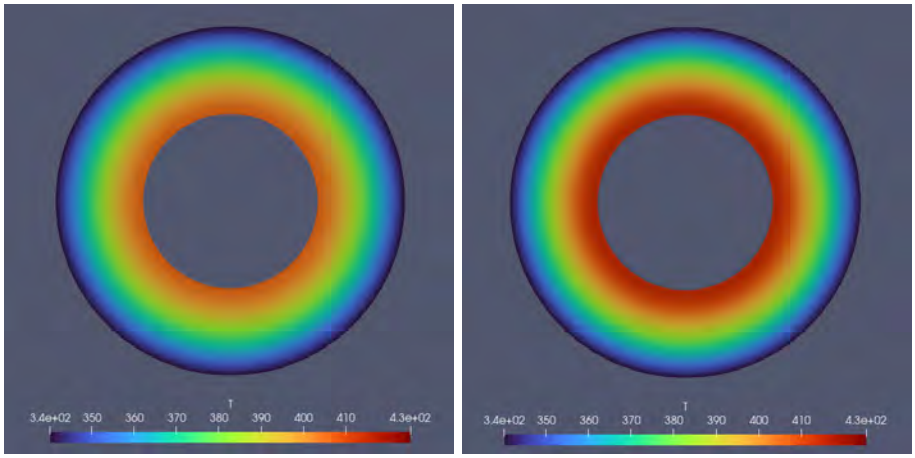

(c) $Br = 1.5$ (d) $Br = 1.75$

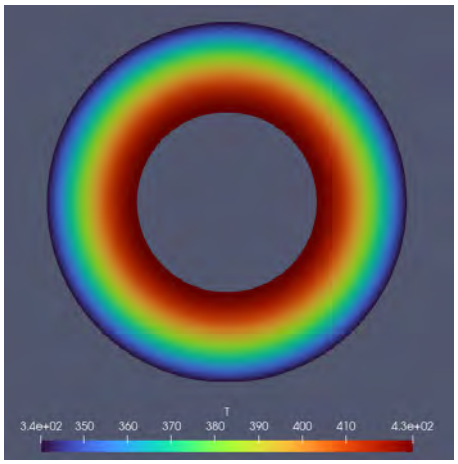

(e) $Br = 2$

Figure 5.11: Temperature profile for $\kappa = 0.5$ and ranging of Br values from 0.5 to 2. In the legend the minimum temperature is $340K$, the maximum is $430K$ and the scaling is $10K$.

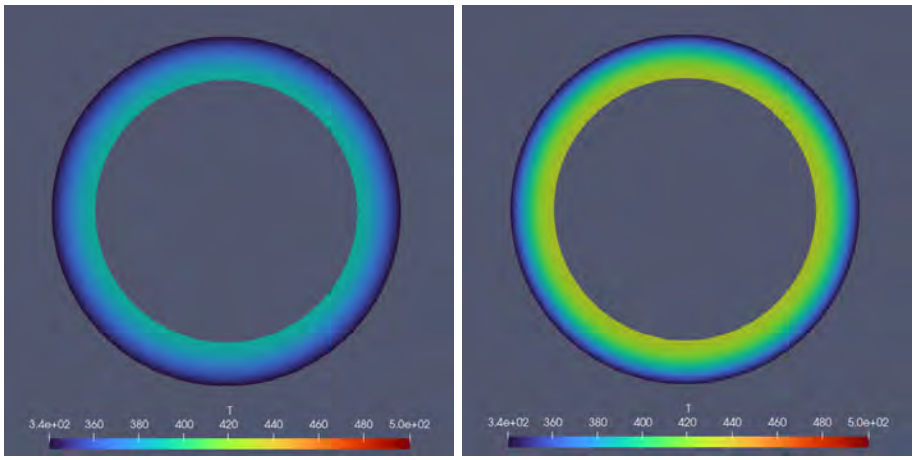

(a) $Br = 0.5$ (b) $Br = 1$

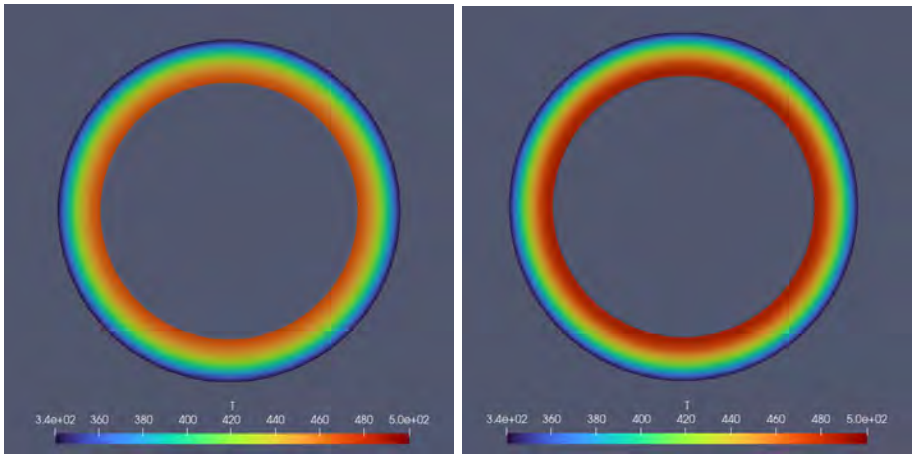

(c) $Br = 1.5$ (d) $Br = 1.75$

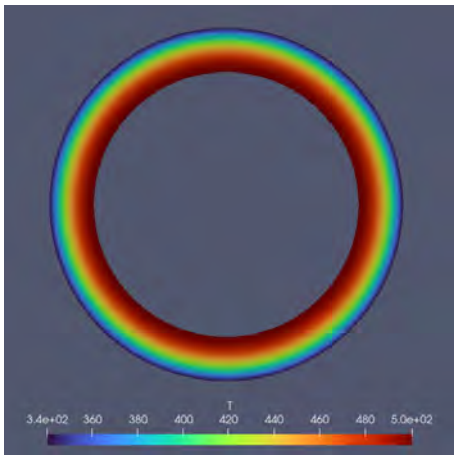

(e) $Br = 2$

Figure 5.12: Temperature profile for $\kappa = 0.75$ and ranging of Br values from 0.5 to 2. In the legend the minimum temperature is $340K$, the maximum is $500K$ and the scaling is $20K$.

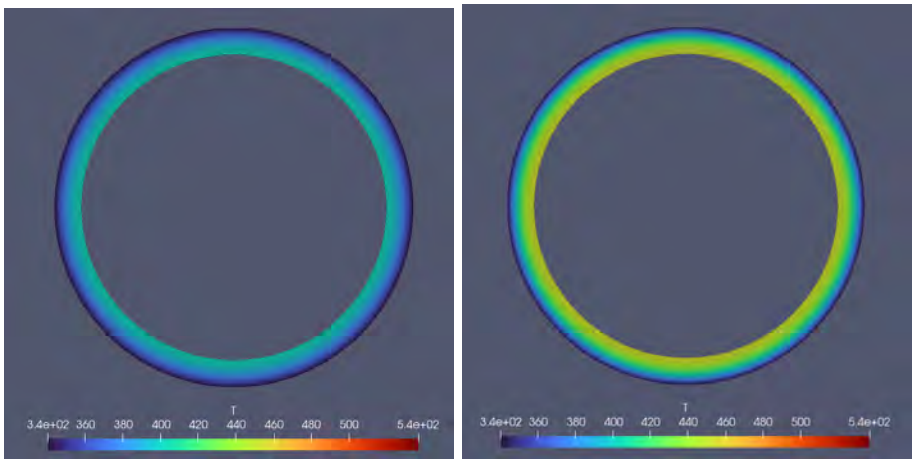

(a) $Br = 0.5$ (b) $Br = 1$

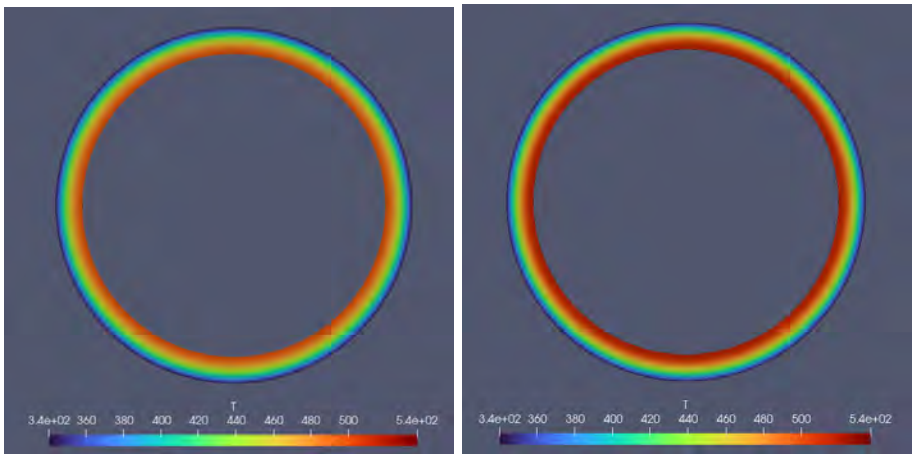

(c) $Br = 1.5$ (d) $Br = 1.75$

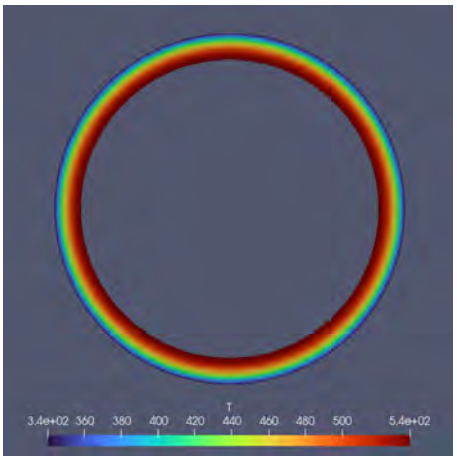

(e) $Br = 2$

Figure 5.13: Temperature profile for $\kappa = 0.85$ and ranging of Br values from 0.5 to 2. In the legend the minimum temperature is $340K$, the maximum is $540K$ and the scaling is $20K$.

Regarding the velocity profile, in the figures 5.14, 5.15 and 5.16 is conducted a comparison of the velocity profiles obtained by the simulations, for different values of κ and Br number.

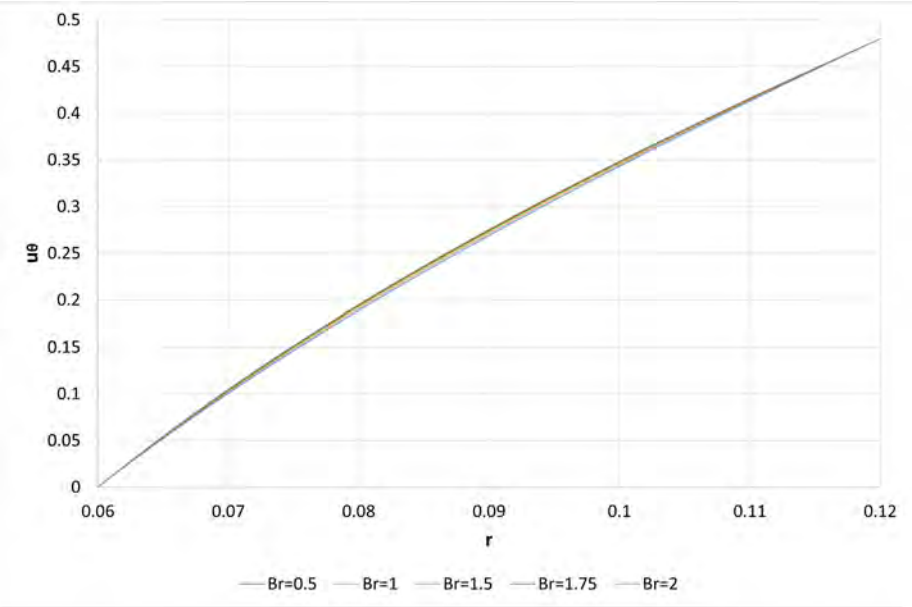

Figure 5.14: Velocity profiles for $\kappa = 0.5$ and ranging of Br values from 0.5 to 2. Where, the y-axis refers to the velocity $u_\theta(m/s)$ and the x-axis to the distance between the cylinders $r(m)$.

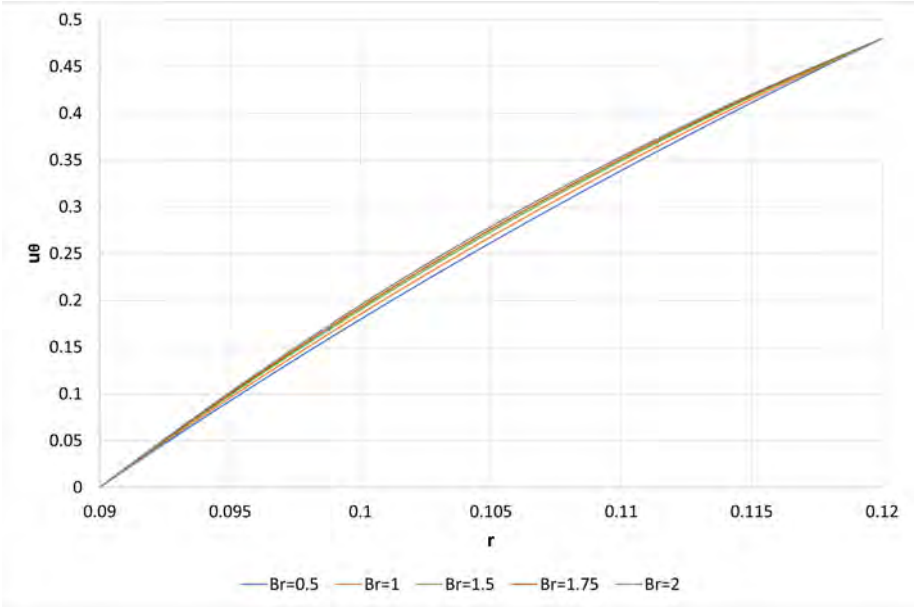

Figure 5.15: Velocity profiles for $\kappa = 0.75$ and ranging of Br values from 0.5 to 2. Where, the y-axis refers to the velocity $u_\theta(m/s)$ and the x-axis to the distance between the cylinders $r(m)$.

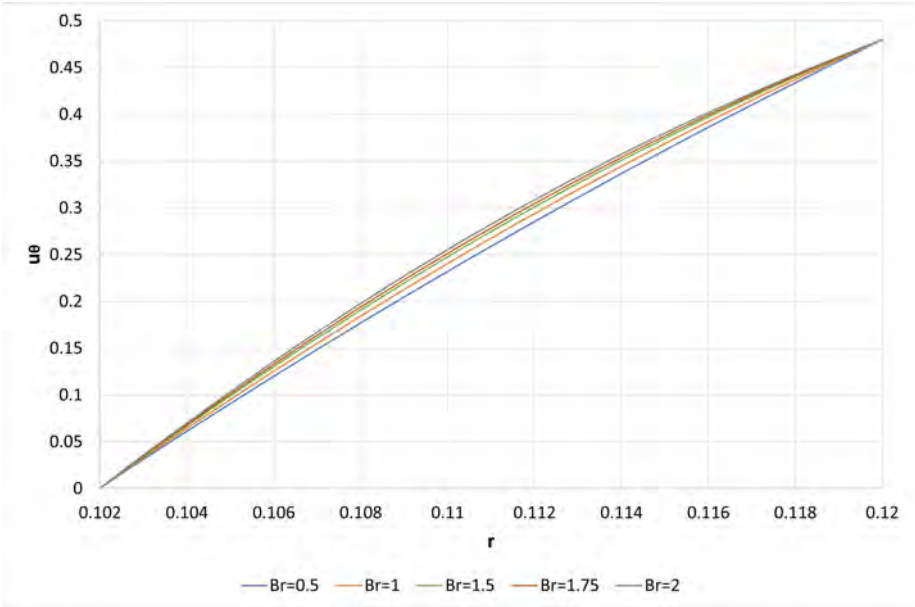

Figure 5.16: Velocity profiles for $\kappa = 0.85$ and ranging of Br values from 0.5 to 2. Where, the y-axis refers to the velocity $u_\theta(m/s)$ and the x-axis to the distance between the cylinders $r(m)$.

From the comparisons above, it is noticeable that as the Br number increases, the velocity profile becomes more parabolic. This alteration is more apparent as the size of the annulus decreases.

Furthermore, is carried out a detailed comparison between the series solution (as described in section 2.3) and the OpenFOAM simulations for the temperature and velocity profile across the annulus.

In figures 5.17, 5.18 and 5.19 is presented the comparison for different values of κ and Br number. Where, the left y-axis refers to the temperature $T(K)$, the right y-axis to the velocity $u_\theta(m/s)$ and the x-axis to the distance $r(m)$ between the two cylinders. The orange and the blue continuous lines indicate, respectively, the temperature and the velocity profiles as obtained from the OpenFOAM simulations. The dotted lines refer to the temperature profile as given by the third-order series solution (2.50) and the velocity profile as given by the second-order series solution (2.35).

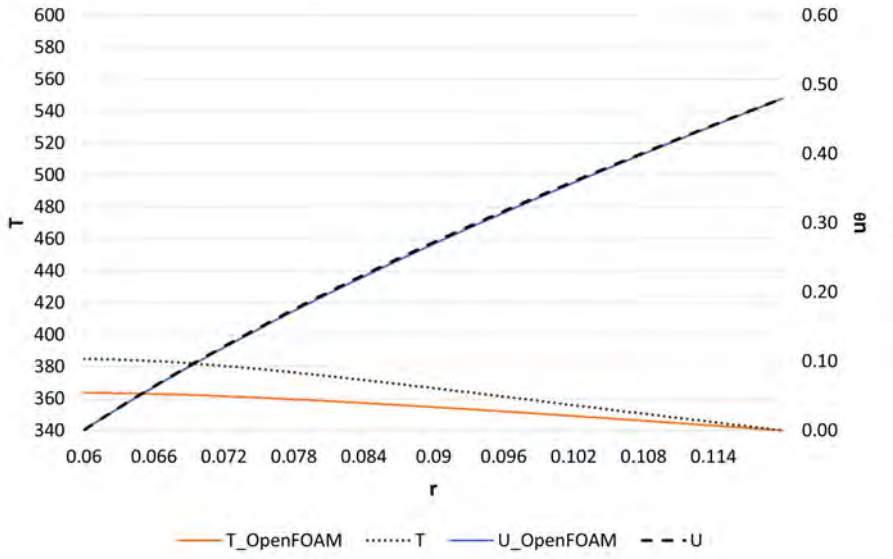

(a) Comparison between series solution and OpenFOAM solution for $\kappa = 0.5$ and $Br = 0.5$. Where, $T(K)$ refers to the temperature, $u_\theta(m/s)$ to the velocity and $r(m)$ to the distance between the cylinders. The continuous lines indicate the profiles as obtained from the simulations and the dotted lines the profiles as given by the series solutions.

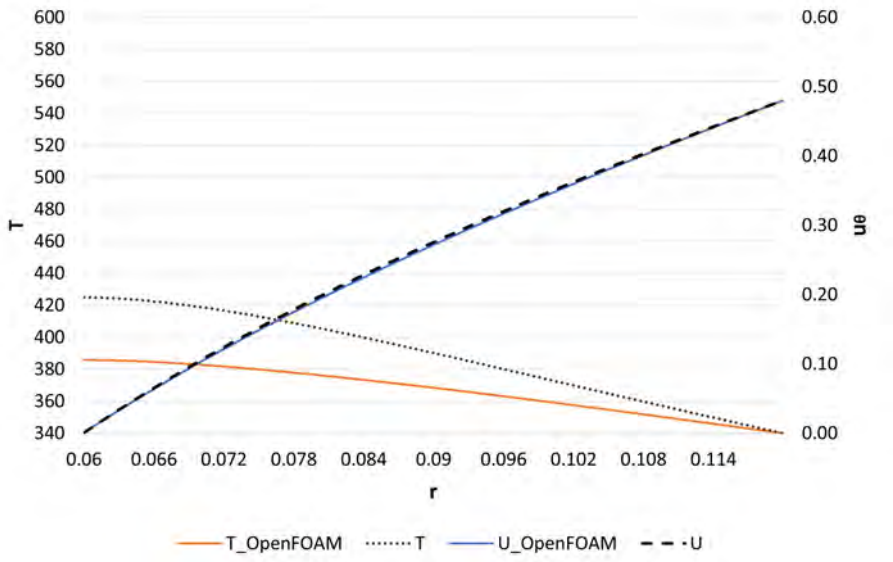

(b) Comparison between series solution and OpenFOAM solution for $\kappa = 0.5$ and $Br = 1$. Where, $T(K)$ refers to the temperature, $u_\theta(m/s)$ to the velocity and $r(m)$ to the distance between the cylinders. The continuous lines indicate the profiles as obtained from the simulations and the dotted lines the profiles as given by the series solutions.

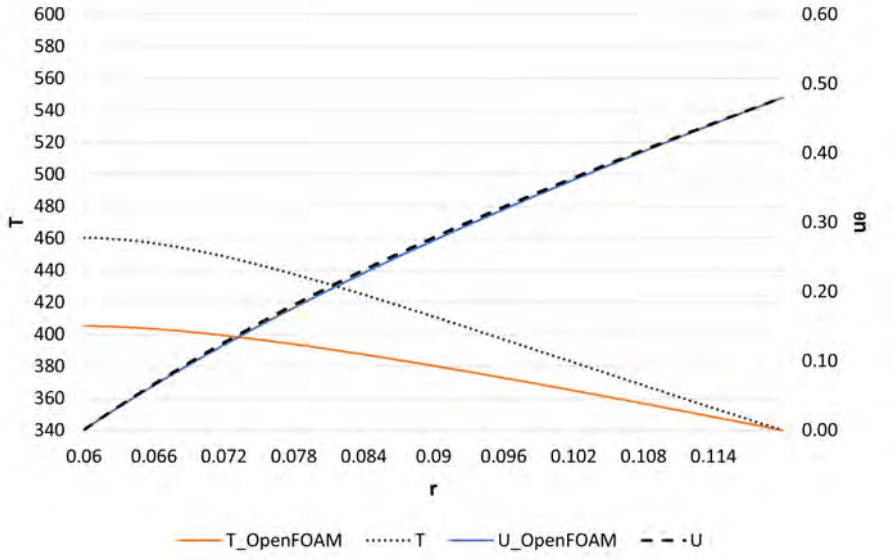

(c) Comparison between series solution and OpenFOAM solution for $\kappa = 0.5$ and $Br = 1.5$. Where, $T(K)$ refers to the temperature, $u_\theta(m/s)$ to the velocity and $r(m)$ to the distance between the cylinders. The continuous lines indicate the profiles as obtained from the simulations and the dotted lines the profiles as given by the series solutions.

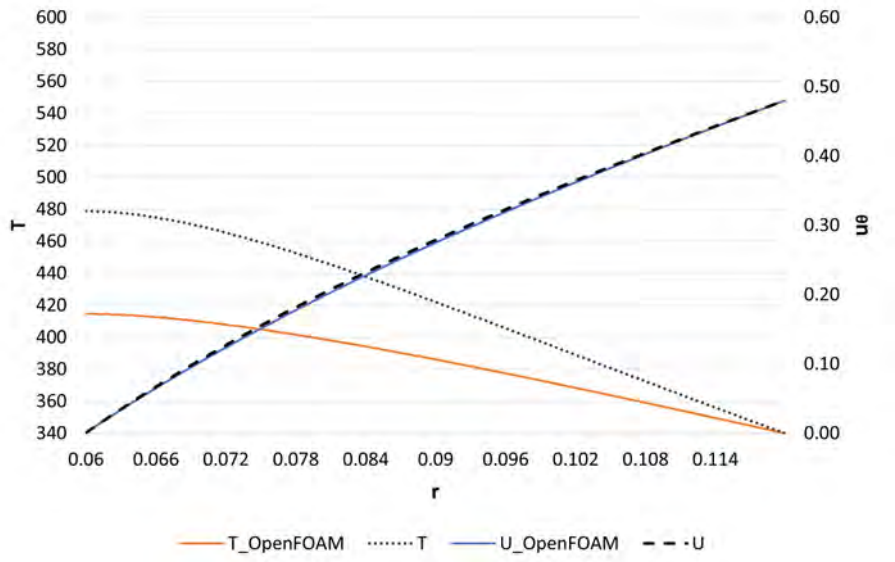

(d) Comparison between series solution and OpenFOAM solution for $\kappa = 0.5$ and $Br = 1.75$. Where, $T(K)$ refers to the temperature, $u_\theta(m/s)$ to the velocity and $r(m)$ to the distance between the cylinders. The continuous lines indicate the profiles as obtained from the simulations and the dotted lines the profiles as given by the series solutions.

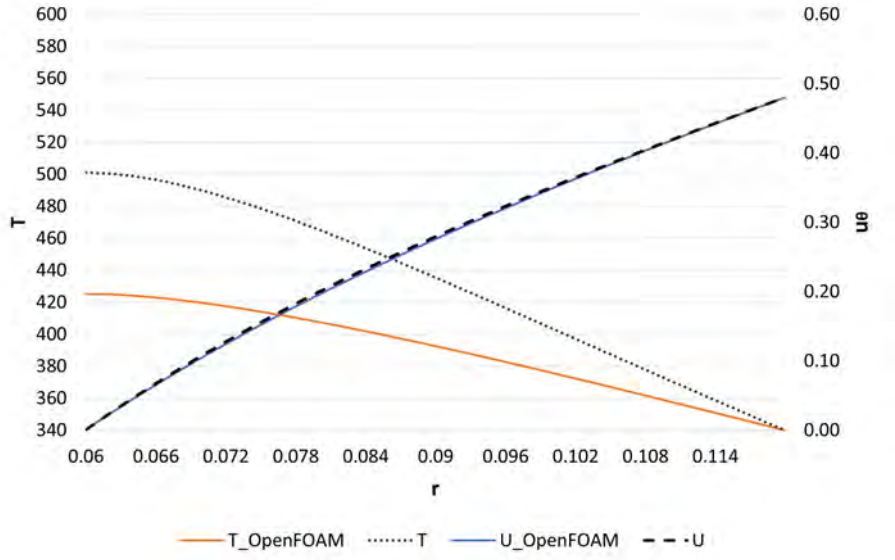

(e) Comparison between series solution and OpenFOAM solution for $\kappa = 0.5$ and $Br = 2$. Where, $T(K)$ refers to the temperature, $u_\theta(m/s)$ to the velocity and $r(m)$ to the distance between the cylinders. The continuous lines indicate the profiles as obtained from the simulations and the dotted lines the profiles as given by the series solutions.

Figure 5.17: Comparison between series solution and OpenFOAM solution for $\kappa = 0.5$ and Br ranging from 0.5 to 2.

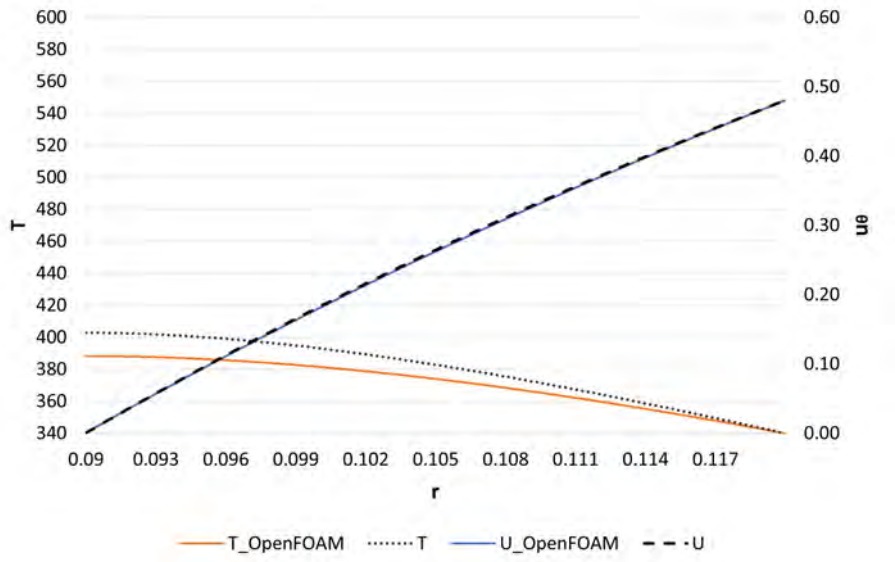

(a) Comparison between series solution and OpenFOAM solution for $\kappa = 0.75$ and $Br = 0.5$. Where, $T(K)$ refers to the temperature, $u_\theta(m/s)$ to the velocity and $r(m)$ to the distance between the cylinders. The continuous lines indicate the profiles as obtained from the simulations and the dotted lines the profiles as given by the series solutions.

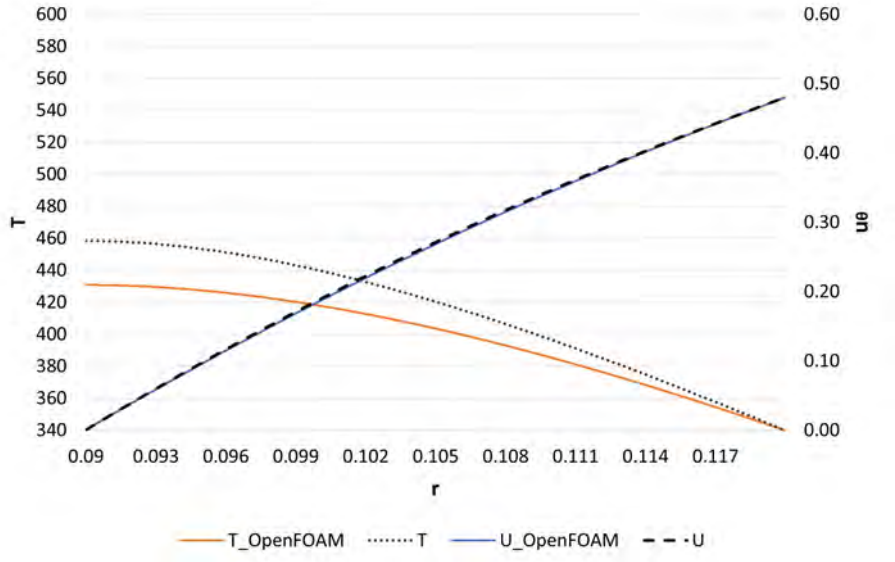

(b) Comparison between series solution and OpenFOAM solution for $\kappa = 0.75$ and $Br = 1$. Where, $T(K)$ refers to the temperature, $u_\theta(m/s)$ to the velocity and $r(m)$ to the distance between the cylinders. The continuous lines indicate the profiles as obtained from the simulations and the dotted lines the profiles as given by the series solutions.

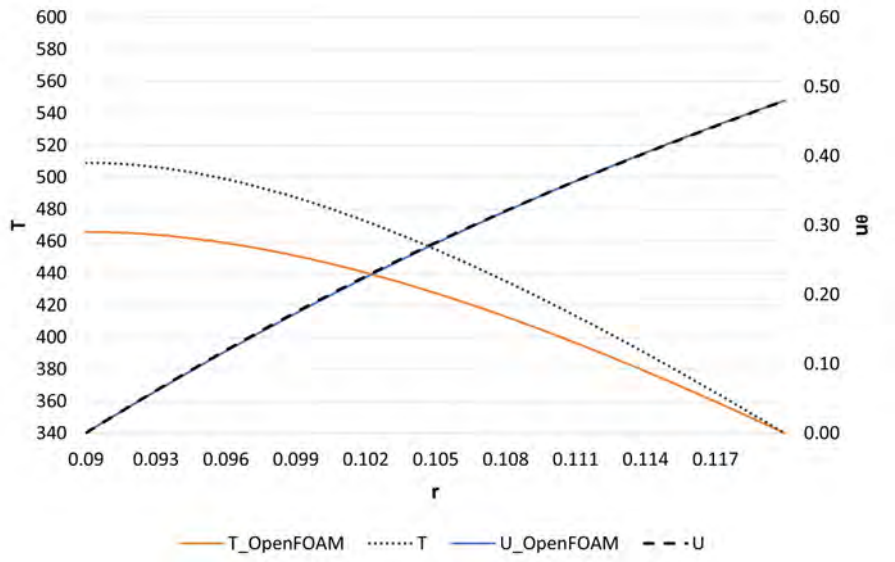

(c) Comparison between series solution and OpenFOAM solution for $\kappa = 0.75$ and $Br = 1.5$. Where, $T(K)$ refers to the temperature, $u_\theta(m/s)$ to the velocity and $r(m)$ to the distance between the cylinders. The continuous lines indicate the profiles as obtained from the simulations and the dotted lines the profiles as given by the series solutions.

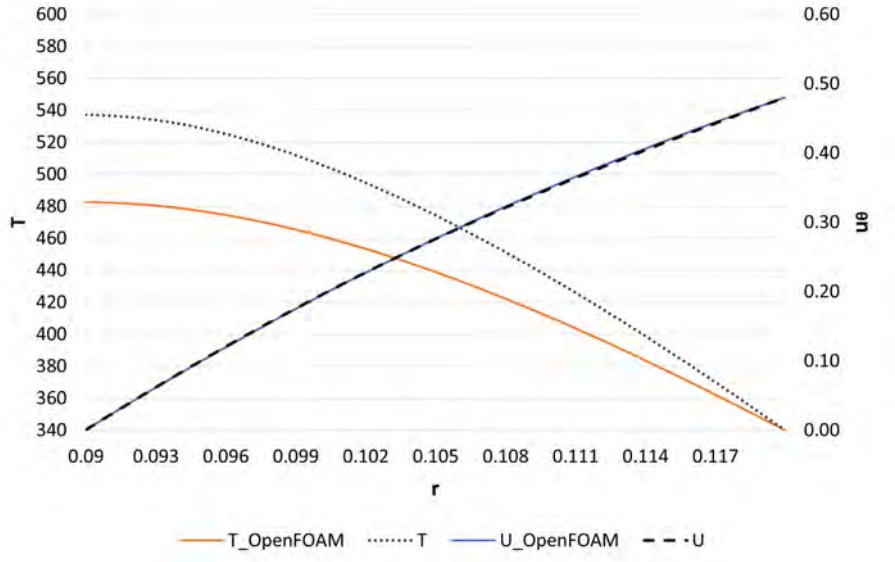

(d) Comparison between series solution and OpenFOAM solution for $\kappa = 0.75$ and $Br = 1.75$. Where, $T(K)$ refers to the temperature, $u_\theta(m/s)$ to the velocity and $r(m)$ to the distance between the cylinders. The continuous lines indicate the profiles as obtained from the simulations and the dotted lines the profiles as given by the series solutions.

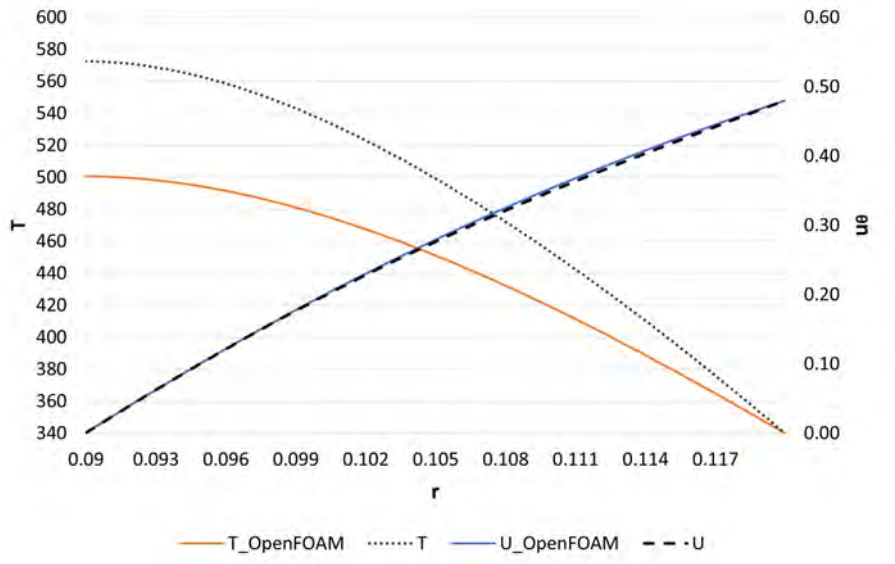

(e) Comparison between series solution and OpenFOAM solution for $\kappa = 0.75$ and $Br = 2$. Where, $T(K)$ refers to the temperature, $u_\theta(m/s)$ to the velocity and $r(m)$ to the distance between the cylinders. The continuous lines indicate the profiles as obtained from the simulations and the dotted lines the profiles as given by the series solutions.

Figure 5.18: Comparison between series solution and OpenFOAM solution for $\kappa = 0.75$ and Br ranging from 0.5 to 2.

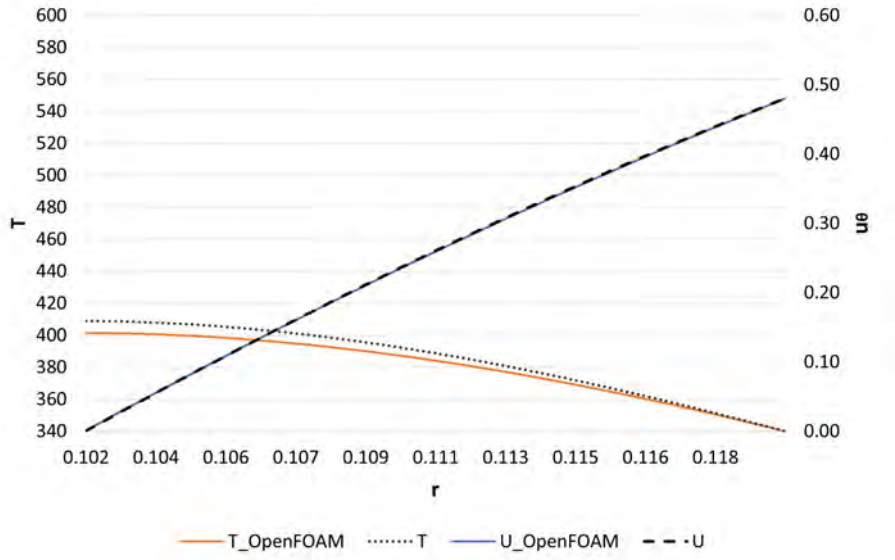

(a) Comparison between series solution and OpenFOAM solution for $\kappa = 0.85$ and $Br = 0.5$. Where, $T(K)$ refers to the temperature, $u_\theta(m/s)$ to the velocity and $r(m)$ to the distance between the cylinders. The continuous lines indicate the profiles as obtained from the simulations and the dotted lines the profiles as given by the series solutions.

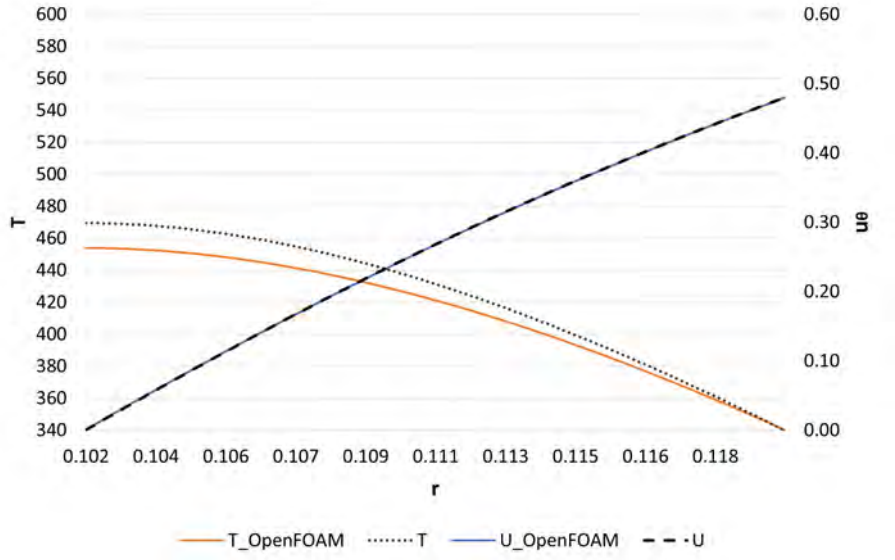

(b) Comparison between series solution and OpenFOAM solution for $\kappa = 0.85$ and $Br = 1$. Where, $T(K)$ refers to the temperature, $u_\theta(m/s)$ to the velocity and $r(m)$ to the distance between the cylinders. The continuous lines indicate the profiles as obtained from the simulations and the dotted lines the profiles as given by the series solutions.

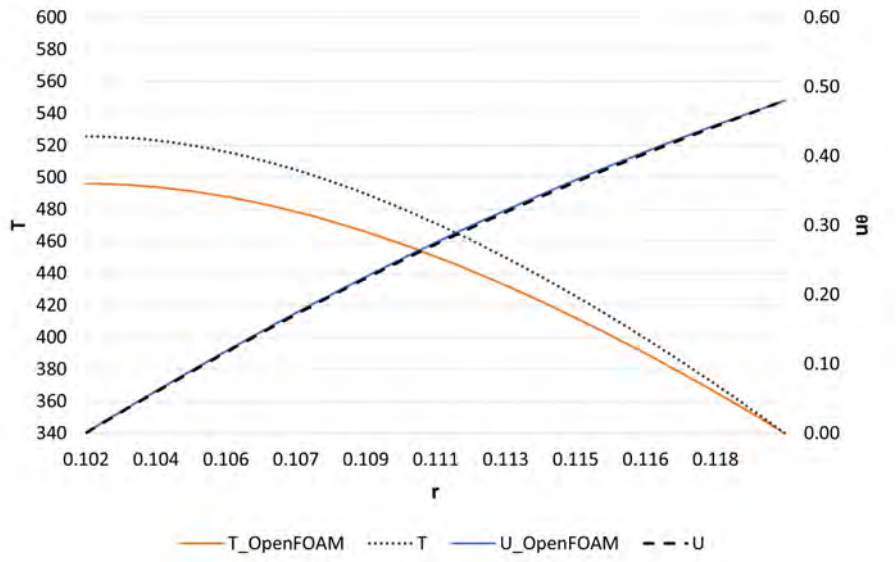

(c) Comparison between series solution and OpenFOAM solution for $\kappa = 0.85$ and $Br = 1.5$. Where, $T(K)$ refers to the temperature, $u_\theta(m/s)$ to the velocity and $r(m)$ to the distance between the cylinders. The continuous lines indicate the profiles as obtained from the simulations and the dotted lines the profiles as given by the series solutions.

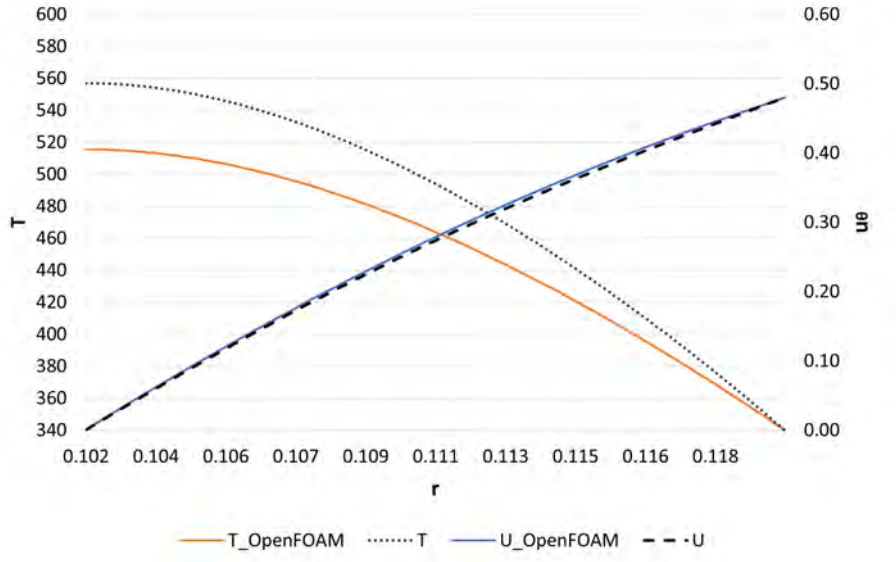

(d) Comparison between series solution and OpenFOAM solution for $\kappa = 0.85$ and $Br = 1.75$. Where, $T(K)$ refers to the temperature, $u_\theta(m/s)$ to the velocity and $r(m)$ to the distance between the cylinders. The continuous lines indicate the profiles as obtained from the simulations and the dotted lines the profiles as given by the series solutions.

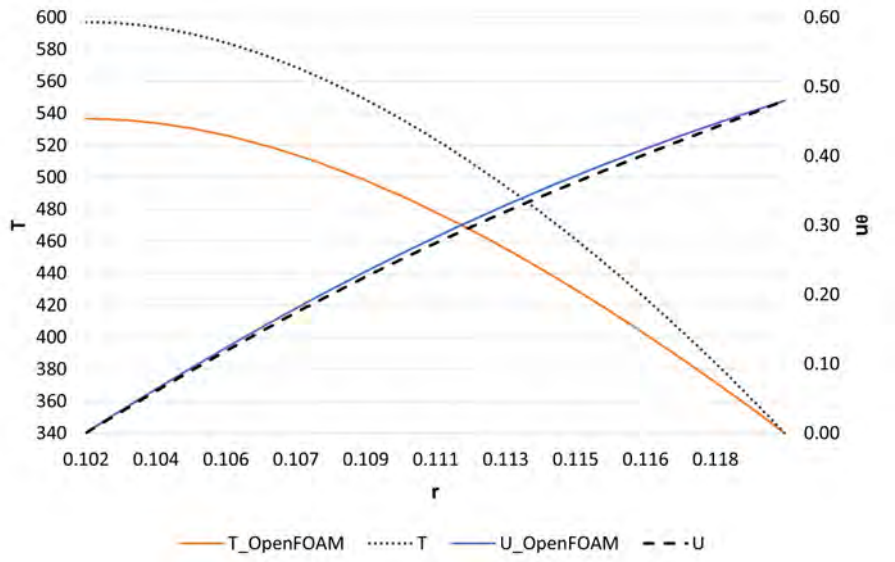

(e) Comparison between series solution and OpenFOAM solution for $\kappa = 0.85$ and $Br = 2$. Where, $T(K)$ refers to the temperature, $u_\theta(m/s)$ to the velocity and $r(m)$ to the distance between the cylinders. The continuous lines indicate the profiles as obtained from the simulations and the dotted lines the profiles as given by the series solutions.

Figure 5.19: Comparison between series solution and OpenFOAM solution for $\kappa = 0.85$ and Br ranging from 0.5 to 2.

From the above comparison can be observed that, the velocity profiles obtained from the series solution and the OpenFOAM simulations are sufficiently identical, with the occurrence of a small deviation for Br values above around 1.5. This deviation is more noticeable as the gap between the cylinders decreases.

Regarding to the temperature, the deviation between the two solutions is clearly more apparent, with its maximum value occurring at the point of maximum temperature. It can be observed that as the Br number increases the deviation becomes more significant. It is shown that the solution is also affected by the geometrical parameter κ, where the discrepancy between the series and the OpenFOAM solution increases with the increase of the annulus. Furthermore, the maximum developed temperature increases with the increase of the radius ratio κ. In the table 3 is presented a more detailed comparison between the maximum temperature as obtained from the simulations and the series solution for the different values of κ and Br number ranging from 0.5 to 2.

	$\kappa = 0.5$			$\kappa = 0.75$			$\kappa = 0.85$		
Br	$T_f(K)$	$T_s(K)$	$\Delta T(K)$	$T_f(K)$	$T_s(K)$	$\Delta T(K)$	$T_f(K)$	$T_s(K)$	$\Delta T(K)$
0.5	363.58	384.71	21.13	388.3	402.83	14.53	401.46	408.83	7.37
1	385.82	424.85	39.03	430.91	458.4	27.49	453.99	469.53	15.54
1.5	405.15	460.28	55.13	465.94	509.15	43.21	496.08	525.60	29.52
1.75	414.66	478.8	64.14	482.55	537.11	54.56	515.67	556.98	41.31
2	425.28	501.08	75.8	500.63	572.45	71.82	536.71	597.18	60.47

Table 3: Maximum temperatures as obtained from the simulations (T_f) and the series (T_s) solution and the difference between them (ΔT) for three different values of κ and a range of values of Br number.

6 CONCLUSIONS

Couette flow can be found in many chemical and mechanical engineering applications. The correct computation of the flow is very important, especially in applications where the fluid properties, as the viscosity, are functions of temperature. In this cases should be carefully considered the heat production due to viscous forces between the fluid elements, a phenomenon known as viscous dissipation. For this, the investigation of the parameters that affect the flow is of great importance.

In this thesis, was considered the flow of materials with viscosity as a polynomial function of temperature. Both geometrical parameters and material properties were investigated. Three different geometries were created, based on the size of the annulus which was expressed by the radius ratio κ. For each geometry, were conducted flow simulations by using the CFD software OpenFOAM, obtaining the velocity and temperature profiles. Furthermore, were presented approximate series solutions up to second-order in Br number for the velocity and third-order for the temperature distribution. An extended comparison between the simulations and the series solutions results was conducted and the factors that affect the flow were examined.

Regarding to the velocity, for a small gap between the cylinders, the profile can be sufficiently approximated by a linear profile. With the increase of the gap, the profile becomes parabolic. Another interesting observation was that the velocity profile becomes more parabolic with the increase of Br number. This variation is more noticeable as the value of the ratio κ increases.

The temperature distribution is also affected by the size of the gap between the cylinders. It was observed that, the maximum developed temperature increases with the increase of the cylinders radius ration κ. Furthermore, for constant annulus size, the point of maximum temperature increases with the increase of Br number.

From the comparison between the simulation's results and the series solution, was shown that the velocity profiles were identical for Br number values up to 1.5. Above that value was occurred a small deviation, which was more apparent for small annulus sizes. However, for the temperature distribution, the deviation was clearly more apparent, especially at the point of maximum temperature. The discrepancy between the two solutions was increasing with the increase of Br number or the increase of the annulus.

Therefore, both the size of the annulus and the Br number are important parameters that can determine the Couette flow development and should be considered.

A APPENDIX A

The coefficients $u_{2\gamma 1}$, $u_{2\gamma 2}$, $u_{2\gamma 3}$, $u_{2\gamma 4}$ of the equation (2.44) can be expressed as:

$$u_{2\gamma 1} = -384(\Lambda_1(\kappa)\beta_1^2 + \Lambda_2(\kappa)\beta_2) \tag{A.1}$$

$$u_{2\gamma 2} = C_0^5 u_{2\gamma 21} + 192 u_{2\gamma 22} \tag{A.2}$$

where,

$$u_{2\gamma 21} = \frac{3}{\kappa^4}\left[(-3\kappa^4 + 12\kappa^2 - 16\ln(\kappa) - 12)\beta_1^2 - (2\kappa^4 - 4 + 4\kappa^2)2\beta_2\right] \tag{A.3}$$

$$u_{2\gamma 22} = \Lambda_3(\kappa)\beta_1^2 - \Lambda_4(\kappa)\beta_2 \tag{A.4}$$

$$u_{2\gamma 3} = \left[\left(\frac{-5\kappa^2 + \kappa^4 + 4 + 12\ln(\kappa)}{\kappa^2(-1+\kappa^2)}\right)3\beta_1^2 + \frac{6\beta_2}{\kappa^2} - 12\beta_2\right] C_0^5 \tag{A.5}$$

$$u_{2\gamma 4} = \left(\beta_1^2 + 4\beta_2\right) C_0^5 \tag{A.6}$$

The $\Lambda_1(\kappa)$, $\Lambda_2(\kappa)$, $\Lambda_3(\kappa)$ and $\Lambda_4(\kappa)$ constants can be obtained as:

$$\Lambda_1(\kappa) = \frac{\kappa^6}{12}\left(\frac{-19\kappa^4 - 12\kappa^4\ln(\kappa) + 4\kappa^6 + 26\kappa^2 + 08\ln(\kappa)\kappa^2 - 48\ln(\kappa)^2\kappa^2 - 96\ln(\kappa) - 96\ln(\kappa)^2 - 11}{(-1+\kappa^2)^7}\right) \tag{A.7}$$

$$\Lambda_2(\kappa) = -\frac{\kappa^6}{6}\left(\frac{4\kappa^4 + 5 + 24\ln(\kappa)^2 + 36\ln(\kappa) - 24\ln(\kappa)\kappa^2 - 9\kappa^2}{(-1+\kappa^2)^6}\right) \tag{A.8}$$

$$\Lambda_3(\kappa) = -\frac{\kappa^6}{6}\left(\frac{5\kappa^8 - 38\kappa^6 + (24\ln(\kappa) + 108)\kappa^4 + (-168\ln(\kappa) - 122 + 48\ln(\kappa)^2)\kappa^2 + 144\ln(\kappa) + 96\ln(\kappa)^2 + 47}{(-1+\kappa^2)^7}\right) \tag{A.9}$$

$$\Lambda_4(\kappa) = -\frac{\kappa^6}{3}\left(\frac{2\kappa^6 - 15\kappa^4 - 17 - 24\ln(\kappa)^2 - 36\ln(\kappa) + 24\ln(\kappa)\kappa^2 + 30\kappa^2}{(-1+\kappa^2)^6}\right) \tag{A.10}$$

B APPENDIX B

The coefficients c_i of the equation (3.3) can be expressed as:

$$c_0 = 0 \tag{B.1}$$

$$c_1 = -\beta_1 \tag{B.2}$$

$$c_2 = -\beta_2 + \beta_1^2 \tag{B.3}$$

$$c_3 = 2\beta_2\beta_1 - \beta_1^3 - \beta_3 \tag{B.4}$$

$$c_4 = \beta_1^4 - 3\beta_1^2\beta_2 + 2\beta_3\beta_1 + \beta_2^2 \tag{B.5}$$

$$c_5 = 4\beta_1^3\beta_2 - \beta_1^5 - 3\beta_3\beta_1^2 - 3\beta_1\beta_2^2 + 2\beta_3\beta_2 \tag{B.6}$$

$$c_6 = \beta_1^6 - 5\beta_1^4\beta_2 + 4\beta_1^3\beta_3 + 6\beta_1^2\beta_2^2 - 6\beta_1\beta_2\beta_3 - \beta_2^3 + \beta_3^2 \tag{B.7}$$

$$c_7 = 6\beta_1^5\beta_2 - \beta_1^7 - 5\beta_1^4\beta_3 - 10\beta_1^3\beta_2^2 + 12\beta_1^2\beta_2\beta_3 + 4\beta_1\beta_2^3 - 3\beta_1\beta_3^2 - 3\beta_2^2\beta_3 \tag{B.8}$$

References

[1] Wikipedia. Taylor-Couette flow. Wikipedia, the free encyclopedia. `https://en.wikipedia.org/wiki/Taylor%E2%80%93Couette_flow`.

[2] Abiodun O Ajibade and Ayuba M Umar. Effects of viscous dissipation and boundary wall thickness on steady natural convection couette flow with variable viscosity and thermal conductivity. *International Journal of Thermofluids*, 7:100052, 2020.

[3] James M White and Susan J Muller. Experimental studies on the stability of newtonian taylor–couette flow in the presence of viscous heating. *Journal of Fluid Mechanics*, 462:133–159, 2002.

[4] Russell J Donnelly. Taylor–couette flow: the early days. *Phys. Today*, 44(11):32–39, 1991.

[5] Lord Rayleigh. On the dynamics of revolving fluids. *Proceedings of the Royal Society of London. Series A, Containing Papers of a Mathematical and Physical Character*, 93(648):148–154, 1917.

[6] Geoffrey Ingram Taylor. Viii. stability of a viscous liquid contained between two rotating cylinders. *Philosophical Transactions of the Royal Society of London. Series A, Containing Papers of a Mathematical or Physical Character*, 223(605-615):289–343, 1923.

[7] JW Lewis. An experimental study of the motion of a viscous liquid contained between two coaxial cylinders. *Proceedings of the Royal Society of London. Series A, Containing Papers of a Mathematical and Physical Character*, 117(777):388–407, 1928.

[8] KW Schwarz, BE Springett, and RJ Donnelly. Modes of instability in spiral flow between rotating cylinders. *Journal of Fluid Mechanics*, 20(2):281–289, 1964.

[9] Donald Coles. Transition in circular couette flow. *Journal of Fluid Mechanics*, 21(3):385–425, 1965.

[10] B Gebhart. Effects of viscous dissipation in natural convection. *Journal of fluid Mechanics*, 14(2):225–232, 1962.

[11] Jacques CJ Nihoul. Nonlinear couette flows with temperature-dependent viscosity. *The Physics of Fluids*, 13(1):203–204, 1970.

[12] Peter C Sukanek and Robert L Laurence. An experimental investigation of viscous heating in some simple shear flows. *AIChE Journal*, 20(3):474–484, 1974.

[13] TD Papathanasiou, KA Caridis, and B Bijeljic. Thermomechanical coupling in frictionally heated circular couette flow. *International journal of thermophysics*, 18(3):825–843, 1997.

[14] Gopal Chandra Hazarika and Jadav Konch. Effects of variable viscosity and thermal conductivity on magnetohydrodynamic free convection dusty fluid along a vertical porous plate with heat generation. *Turkish Journal of Physics*, 40(1):52–68, 2016.

[15] RA Kareem and SO Salawu. Variable viscosity and thermal conductivity effect of soret and dufour on inclined magnetic field in non-darcy permeable medium with dissipation. *British Journal of Mathematics & Computer Science*, 2(3):1–12, 2017.

[16] TaiwoS Yusuf and MichaelO Oni. Entropy generation under the influence of radial magnetic field and viscous dissipation of generalized couette flow in an annulus. *Propulsion and Power Research*, 7(4):342–352, 2018.

[17] Pranab Kumar Mondal and Somchai Wonwises. Assesment of thermodynamic irreversibility in a micro-scale viscous dissipative circular couette flow. *Entropy*, 20(1):50, 2018.

[18] Basant K Jha and Peter B Malgwi. Couette flow and heat transfer of heat-generating/absorbing fluid in a rotating channel in presence of viscous dissipation. *Arab Journal of Basic and Applied Sciences*, 27(1):67–74, 2020.

[19] Sarah Shabbir, Seamus D Garvey, Sam M Dakka, and Benjamin C Rothwell. Heat transfer of couette flow in micro-channels: an analytical model of seals. 2020.

[20] TD Papathanasiou. Circular couette flow of temperature-dependent materials: Asymptotic solutions in the presence of viscous heating. *Chemical engineering science*, 52(12):2003–2006, 1997.

[21] TD Papathanasiou. Explicit corrections for the effect of viscous heating in circular couette viscometers. *International journal of thermophysics*, 19(1):71–88, 1998.

[22] Caridis KA, B Louwagie, and Papathanasiou TD. Viscous heating in planar couette flow: series solutions for temperature-sensitive fluids. *Journal of chemical engineering of Japan*, 30(1):123–136, 1997.

[23] OpenFOAMwiki. Simplefoam. `https://openfoamwiki.net/index.php/SimpleFoam`.

[24] Christophe Geuzaine and Jean-François Remacle. Gmsh: A 3-d finite element mesh generator with built-in pre-and post-processing facilities. *International journal for numerical methods in engineering*, 79(11):1309–1331, 2009.